



TECHNISCHE  
UNIVERSITÄT  
WIEN



institute of  
telecommunications

---

# Beamforming for LTE MBMS/MBSFN

---

MASTER THESIS

*Author:*

Illia Safulin

Staargasse 8/46, 1140 Wien, Austria

*Main supervisor:*

Univ.Prof. Dipl.-Ing. Dr.techn. Markus Rupp

*Second supervisor:*

Univ.Ass. Dipl.-Ing. Dr.techn. Stefan Schwarz

Technische Universität Wien

Electrical Engineering and Information Technology

Institute of Telecommunications

May 20, 2016



# Declaration of Authorship

I, Illia Safiulin, declare that this thesis titled, 'Beamforming for LTE MBM-S/MBSFN' and the work presented in it are my own, and the work done by other authors is appropriately cited.

Illia Safiulin  
May 20, 2016



# Abstract

## Beamforming for LTE MBMS/MBSFN

by Illia Safiulin

Multimedia Broadcast Multicast Service (MBMS) is a feature of the Third Generation Partnership Project's (3GPP's) LTE to support multicast transmission to multiple users in parallel, enabling more efficient utilization of network resources, e.g., for video broadcasting or common messages. MBMS is mostly considered in combination with Multimedia Broadcast Single Frequency Network (MBSFN), which further enables multicasting over multiple base stations, effectively forming a single frequency network. In this diploma thesis, efficient beamforming algorithms are devised for MBMS/MBSFN and their employment in vehicular communication, especially road safety applications, are investigated. These algorithms are intended to decrease the transmission latency of road safety messages thereby increasing the performance of data transmission within the MBSFN area and improving network utilization. The algorithms were implemented within an LTE compliant simulation framework.

In the first chapter, an introduction to LTE MBSFN networks is given and basics of vehicular communication are shortly described. The aim of this chapter is to describe main architectural nodes introduced by MBSFN and provide insight into road safety applications. It is important to clarify which unique peculiarities experience road safety applications and how and why MBSFN can be used in these circumstances.

Chapter 2 is devoted to an introduction of the basics of OFDM and the technique which allows to model Inter Carrier Interference (ICI). Networks with highly mobile terminals suffer from Doppler shifts, which could cause significant performance degradation. In order to simulate such effects commonly highly complex fast-fading simulations are performed. Due to complexity reasons fast-fading simulations usually are not an option in system level simulations. Nevertheless, in order to have precise modelling, these effects should be considered. In this chapter an efficient and precise technique to mimic fast-fading behaviour is explained and verification results are presented.

In Chapter 3 the physical layer of MBSFN transmission is presented as well as additional mathematical techniques from the area of convex optimization. Additionally, the main performance metrics are explained, which are used to compare the efficiency of standard defined techniques to more advanced concepts introduced in this chapter.

In Chapter 4 simulation results and achieved improvements are shown. The performance of the standard defined transmission in terms of latency and cell resource utilization are compared with results, obtained with algorithms described in previous

---

chapters. Additionally possible gains of MBSFN networks in case of big number of multicast users are provided and explained.

Finally Chapter 5 concludes the results, explains strong and weak parts of the proposed algorithm and sheds a light onto questions which require further investigation.

# Acknowledgements

My first words of gratitude I want to dedicate to my supervisor, Prof. Markus Rupp.  
It was he who believed in my abilities and helped to realize my aspirations.

Also I would like to thank my second supervisor Dr.techn. Stefan Schwarz, who always  
led and assisted mein my research work.

My numerous thanks also go to my colleagues at the LTE Group.

Last but most important, I would like to thank my family, especially my parents, for  
supporting me throughout my studying and my life in general. Without their help and  
efforts I would never have achieved all this.

*Моя семья, спасибо вам большое, за все те слова поддержки, за все  
то, что вы для меня сделали. Я буду всю жизнь благодарен вам за  
это. Еще раз огромное спасибо!*





# Contents

<b>Declaration of Authorship</b>	<b>iii</b>
<b>Abstract</b>	<b>v</b>
<b>Acknowledgements</b>	<b>vii</b>
<b>Contents</b>	<b>viii</b>
<b>List of Figures</b>	<b>xi</b>
<b>List of Tables</b>	<b>xiii</b>
<b>Abbreviations</b>	<b>xv</b>
<b>1 Introduction to LTE MBSFN and Road Safety Applications</b>	<b>1</b>
1.1 LTE MBSFN . . . . .	1
1.2 LTE MBMS Architecture and Overall Channel Structure . . . . .	3
1.3 Road Safety Applications . . . . .	6
1.4 Conclusions . . . . .	9
<b>2 Theoretical Basics of OFDM and ICI Modelling</b>	<b>11</b>
2.1 Introduction to Physical layer of LTE . . . . .	11
2.2 Analytical ICI Model . . . . .	15
2.2.1 Extension to MIMO Transmissions . . . . .	16
2.2.2 Performance Evaluation . . . . .	17
2.3 Conclusions . . . . .	19
<b>3 Physical Layer of LTE MBSFN</b>	<b>21</b>
3.1 System Model . . . . .	21
3.2 Multicast Transmit Beamforming . . . . .	22
3.2.1 Beamformer Randomization . . . . .	24
3.3 Performance Metrics . . . . .	25

3.3.1	Latency Evaluation . . . . .	25
3.3.2	Network Utilization . . . . .	27
3.4	CQI Adaptation . . . . .	27
3.5	Conclusions . . . . .	29
<b>4</b>	<b>Performance Evaluation</b>	<b>31</b>
4.1	Description of Simulation Setup . . . . .	31
4.2	Performance with 4x1 Antenna Configuration . . . . .	35
4.3	Performance with 8x1 Antenna Configuration . . . . .	38
4.4	Utilization . . . . .	40
4.5	Conclusions . . . . .	41
<b>5</b>	<b>Conclusions</b>	<b>43</b>
<b>A</b>	<b>Detailed description of the applied algorithm</b>	<b>45</b>
	<b>Bibliography</b>	<b>49</b>

# List of Figures

1.1	Broadcast vs. unicast transmission. (a) Broadcast. (b) Unicast. . . . .	2
1.2	Structure of LTE MBMS architecture. <i>Source: 4G LTE/LTE-Advanced for Mobile Broadband.</i> . . . . .	3
1.3	Structure of LTE MBMS downlink channel mapping. . . . .	4
1.4	Resource-block structure and reference-signal structure for MBSFN transmission. <i>Source: 4G LTE/LTE-Advanced for Mobile Broadband.</i> . . . . .	5
1.5	Resource-block structure for MBSFN subframes, assuming normal cyclic prefix for the control region. <i>Source: 4G LTE/LTE-Advanced for Mobile Broadband.</i> . . . . .	5
1.6	Road fatalities and vehicle kilometres travelled in nine OECD countries. <i>Source: OECD International Road and Traffic Accident Database.</i> . . . . .	6
1.7	Illustration of different technologies supporting vehicular communication. <i>Source:Kapsch</i> . . . . .	9
2.1	Frame structure of 3GPP LTE. . . . .	12
2.2	Comparison of BLER between fast-fading and block-fading simulation with shortened block-fading length. Simulations of block-fading channels with block fading length of 1, 3, 4, 7 and 14 OFDM symbols are considered. . . . .	17
2.3	Justification of ICI abstraction model at 2 GHz center frequency. Simulations of block-fading channels with block fading length of 1, 3, 4, 7 and 14 OFDM symbols are considered. . . . .	18
2.4	Comparison of $4 \times 2$ MIMO transmissions with system and link level simulations. . . . .	19
2.5	Comparison of $4 \times 4$ MIMO transmissions of fast-fading channel and slow fading channel+ ICI noise. . . . .	19
3.1	Explanation of latency calculation. . . . .	25
3.2	Utilization of cell resources for different number of UEs. . . . .	28
3.3	Comparison of utilization of cell resources for 21 and 49 UEs . . . . .	28
4.1	Illustration of simulated network. . . . .	34
4.2	Latency distribution of baseline scenario with $1 \times 1$ transmission and 3 car UEs per base station. . . . .	35
4.3	Comparison of latency distribution in case of $4 \times 1$ transmission and total number of 21 multicast UEs in MBSFN area. . . . .	36
4.4	Comparison of latency distribution in case of $4 \times 1$ transmission and total number of 42 multicast UEs in MBSFN area. . . . .	37

4.5	Comparison of achievable with multicast beamforming SINR values for different number of multicast UEs per base station in case of 4 antennas per base station. . . . .	38
4.6	Comparison of latency distribution in case of $8 \times 1$ transmission and total number of 21 multicast UEs in MBSFN area. . . . .	39
4.7	Comparison of latency distribution in case of $8 \times 1$ transmission and total number of 42 multicast UEs in MBSFN area. . . . .	40
4.8	Comparison of achievable with multicast beamforming SINR values for different number of multicast UEs per base station in case of 8 antennas per base station. . . . .	41

# List of Tables

1.1	Safety message requirements and use cases. . . . .	8
4.1	Simulation Parameters . . . . .	33
4.2	Comparison of achievable SINRs with beamforming for $4 \times 1$ antenna configuration and different number of multicast UEs. . . . .	37
4.3	Comparison of achievable SINRs with beamforming for $8 \times 1$ antenna configuration and different number of multicast UEs. . . . .	39
4.4	Final comparison of cell resources consumed by road safety messages. Baseline scenario as well as $4 \times 1$ and $8 \times 1$ with different number of multicast UEs are considered . . . . .	41
4.5	Final comparison of mean transmission latency between performance of standard LTE MBSFN transmission and more advanced approaches for different number of car UEs in the network. . . . .	42



# Abbreviations

<b>3GPP</b>	Third Generation Partnership Project
<b>BM-SC</b>	Broadcast Multicast Service Center
<b>BSM</b>	Basic Safety Message
<b>CAM</b>	Cooperative Awareness Message
<b>CEN</b>	European Committee for Standardization
<b>CP</b>	Cyclic Prefix
<b>CQI</b>	Channel-Quality Indicator
<b>DENM</b>	Decentralized Environmental Notification Message
<b>DL</b>	Downlink
<b>DFT</b>	Discrete Fourier Transform
<b>eMBMS</b>	Evolved Multimedia Broadcast Multicast Services
<b>eNodeB</b>	E-UTRAN NodeB
<b>ETSI</b>	European Telecommunications Standards Institute
<b>FDD</b>	Frequency Division Duplex
<b>HARQ</b>	Hybrid Automatic Repeat Request
<b>ICI</b>	Inter Carrier Interference
<b>IDFT</b>	Inverse DFT
<b>IEEE</b>	Institute of Electrical and Electronics Engineers
<b>IP</b>	Internet Protocol
<b>ISI</b>	Intersymbol Interference
<b>ITC</b>	Intelligent Transportation Systems
<b>LTE</b>	Long Term Evolution
<b>MBMS</b>	Multimedia Broadcast/Multicast Service
<b>MBMS-GW</b>	Multimedia Broadcast/Multicast Service Gateway
<b>MBSFN</b>	Multicast-Broadcast Single Frequency Network
<b>MCE</b>	Multi-cell/multicast Coordination Entity

<b>MCH</b>	Multicast Channel
<b>MCCH</b>	Multicast Control Channel
<b>MCS</b>	Modulation-and-Coding Scheme
<b>MIMO</b>	Multiple-Input Multiple-Output
<b>MME</b>	Mobility Management Entity
<b>MNO</b>	Mobile Network Operator
<b>MTCH</b>	Multicast Traffic Channel
<b>NP</b>	Non-deterministic Polynomial
<b>OECD</b>	Organisation for Economic Cooperation and Development
<b>OFDM</b>	Orthogonal Frequency-Division Multiplexing
<b>OFDMA</b>	Orthogonal Frequency-Division Multiple Access
<b>OBU</b>	On-Board Units
<b>PMCH</b>	Physical Multicast Channel
<b>QoS</b>	Quality-of-Service
<b>RB</b>	Resource Block
<b>RE</b>	Resource Element
<b>RLC</b>	Radio Link Control
<b>RSU</b>	Road-Side infrastructure Units
<b>SDR</b>	Semidefinite Relaxation
<b>SINR</b>	Signal-to-Interference-and-Noise Ratio
<b>SISO</b>	Single-Input and Single-Output
<b>SNR</b>	Signal-to-Noise Ratio
<b>TX</b>	Transmitter
<b>UE</b>	User Equipment
<b>UMTS</b>	Universal Mobile Telecommunications System
<b>UTRA</b>	Universal Terrestrial Radio Access
<b>V2I</b>	Vehicle-to-Infrastructure
<b>V2V</b>	Vehicle-to-Vehicle
<b>V2X</b>	Vehicle-to-X
<b>WSSUS</b>	Wide-Sense Stationary Uncorrelated Scattering



# Chapter 1

## Introduction to LTE MBSFN and Road Safety Applications

### 1.1 LTE MBSFN

Delivery of broadcast/multicast services in a mobile-communication system means that the same information is to be provided to multiple terminals simultaneously, often delivered over a large number of cells. The broadcast/multicast information may be a TV streaming, system updates, information about weather conditions, common messages for specific group of users or any other kind of information that, at a given time, should be delivered to large number of different mobile terminals.

When the same information is to be provided to multiple terminals within a cell it is usually beneficial to provide this information as a single “broadcast” radio transmission covering the entire cell and simultaneously being received by all relevant terminals, as shown in Figure 1.1a, rather than providing the information by means of individual transmissions to each terminal, as it is done in standard unicast transmission, which is shown in Figure 1.1b. Broadcast transmission according to Figure 1.1a also has to support the worst-case terminals, including terminals at the cell edge. It should be noted that it will be relative costly in terms of the base-station transmit power to provide sufficient broadcast-service data rates. Additionally, taking into account the limited Signal-to-Noise Ratio (SNR) that can be achieved at the cell edge, the achievable broadcast data rates may be relatively limited, especially in the case of large cells. There are couple of ways to increase the efficiency, one of which is to reduce the cell size, thereby increasing the cell-edge receive power. However, this will increase the number of cells to cover a certain area, which is undesirable for the network operators from a cost-of-deployment point of view. As discussed above, the utilization of broadcast/multicast services in a mobile network typically implies that identical information is to be provided over a large number of cells. Fortunately in such case, the terminals at the cell edge

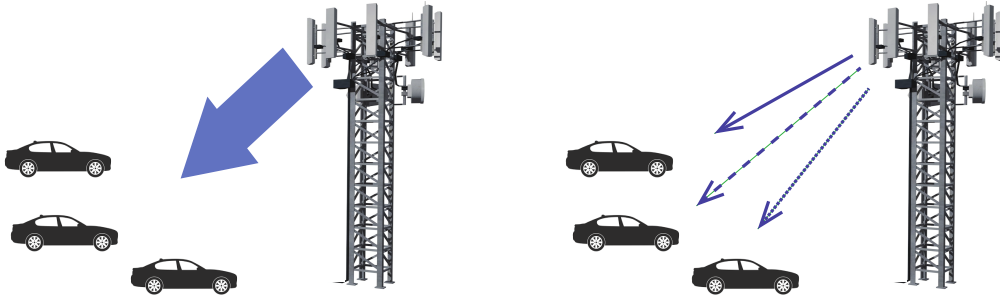


FIGURE 1.1: Broadcast vs. unicast transmission. (a) Broadcast. (b) Unicast.

can utilize the received signals from broadcasting cells when detecting/decoding the broadcast data and treat it as a useful signal. This can be achieved if the broadcast transmissions from different cells are truly identical and transmitted into the same time-frequency resource blocks. In this case, the transmissions received from multiple cells will appear as a transmission from single base station, which suffers from multipath propagation. The transmission of identical time-aligned signals from multiple cells, especially in the case of delivery of broadcast/multicast services, is sometimes referred to as Single-Frequency Network (SFN) operation [1].

In the case of time-aligned transmissions from multiple cells, the inter-cell interference due to transmissions in neighboring cells will be replaced by signal corruption due to time dispersion. If the Orthogonal Frequency-Division Multiplexing (OFDM) cyclic prefix covers the main part of this “time dispersion”, the achievable broadcast data rates are only limited by noise, implying enhancement into Signal-to-Interference-and-Noise Ratio (SINR). Furthermore, the OFDM receiver does not need to explicitly identify the cells to be soft combined.

Thereby Third Generation Partnership Project (3GPP) has introduced Multimedia Broadcast/Multicast Service (MBMS) as a means to broadcast and multicast information to users in Release 6 of Universal Mobile Telecommunications System (UMTS) [2]. MBMS enables to broadcast/multicast information in 3G networks, similar to classical radio/TV broadcast networks, targeting mobile TV as the main service offered. Development of MBMS has continued within 4G Long Term Evolution (LTE), evolving the technology to Evolved Multimedia Broadcast Multicast Services (eMBMS). eMBMS supports multicasting not only from single base stations, but even from multiple strictly time- and frequency-synchronized base stations, forming a so-called MB-SFN area. In the current Release 12 of UMTS LTE, MBMS/MBSFN is restricted to single antenna transmission; however, discussions are ongoing within 3GPP to enable multi-antenna support in future releases. Additionally, MBMS/MBSFN transmission can enhance network efficiency, because common information can be delivered highly resource and cost effective to many users in parallel. Recent interest in the technology by network operators and equipment manufacturers exists especially in the context

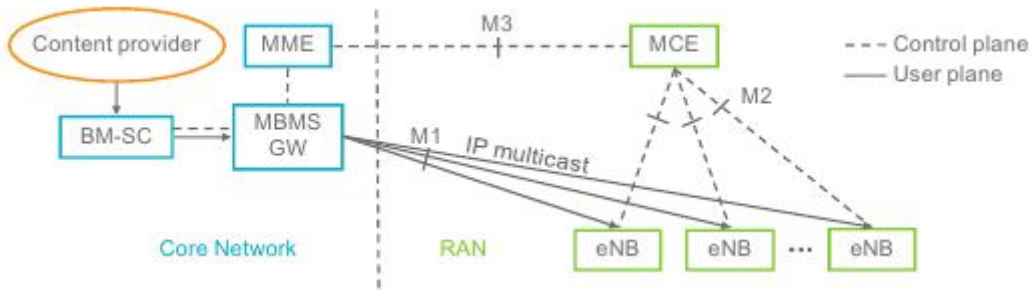


FIGURE 1.2: Structure of LTE MBMS architecture.  
Source: 4G LTE/LTE-Advanced for Mobile Broadband.

of venue casting [3], that is, multicasting/broadcasting at local events. This is confirmed by several technology trials conducted at sport events, such as, football games and car racing [4–6]. At such events, MBMS can be utilized to enhance the experience of spectators by providing additional information, e.g., live video feeds from inside race cars [5] or slow-motions of highlight scenes. Other applications envisioned include software/firmware/operating-system updates for mobile Internet of Things devices [7] as well as broadcasting of road safety related information to vehicles on highways and motorways [8, 9].

## 1.2 LTE MBMS Architecture and Overall Channel Structure

In order to utilize enhancement into SINR, MBSFN transmission requires utilization of the same set of radio resources along with time synchronization among the cells within the MBSFN area. To handle such coordination, the so called Multi-cell/multicast Coordination Entity (MCE) was introduced as a new logical node in the radio-access network. The main task of MCE is allocation of radio resources and transmission parameters between base stations within the MBSFN area (management of control plane). As shown in Figure 1.2, the MCE can control multiple UTRAN NodeBs (eNodeBs). Introduction of the MBSFN mode also affected the core network: new entities, such as a Broadcast Multicast Service Center (BM-SC), MBMS gateway (MBMS-GW) and Mobility Management Entity (MME) were presented. BM-SC is responsible for the overall configuration of the data flow through the core network. The MBMS-GW, from the other side, is a logical node processing multicast of Internet Protocol (IP) packets from the BM-SC to all eNodeBs attached to MBSFN area. Finally, MME allows to manage session control signalling to eNodeBs. Such network architecture allows to utilize multicast capabilities of IP packets, which leads to significant savings in the transport network.

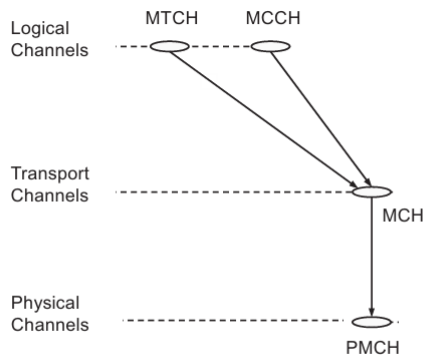


FIGURE 1.3: Structure of LTE MBMS downlink channel mapping.

As the MBSFN mode requires a particular architecture in LTE networks, a new channel structure with specific capabilities was introduced for MBMS transmission. The overall channel structure is depicted in Figure 1.3. A particular physical-channel type, called Physical Multicast Channel (PMCH), is specified for MBSFN transmission, which has specific resource-block structure and reference symbols allocation, depicted in Figure 1.4. These reference symbols are transmitted at the same time–frequency position and with the same values by means of MBSFN over the group eNodeBs that constitute the MBSFN area. Hence, a channel estimation using these reference symbols can be efficiently implemented and will be able to correctly represent the overall channels corresponding to the multicast transmissions. It should be noted that, in MBSFN subframes only the reference signals in the two first OFDM symbols of the subframe, corresponding to the control region of the MBSFN subframe, are actually transmitted. Thus, there is no transmission of cell-specific reference signals within the MBSFN part of the MBMS subframe.

Additionally, a new transport channel, the so called Multicast Channel (MCH), was introduced. MCH is used to support MBMS transmission and can be characterized by a semi-static transport format and scheduling. Transmission of MBMS data has its own logical-downlink channel, specified in LTE, the so called Multicast Traffic Channel (MTCH), which is used for downlink transmission of MBMS data. This logical channel type corresponds to a specific MBMS service. If the number of services to be provided in an MBSFN area is large, multiple MTCHs can be configured. Obviously, as no acknowledgements are transmitted by the terminals, no Radio Link Control (RLC) retransmissions can be used and consequently the RLC unacknowledged mode is used. At the same time, Multicast Control Channel (MCCH) is specified, which is the logical channel type used to carry control information necessary for reception of a certain MBMS service, including the subframe allocation and Modulation-and-Coding Scheme (MCS) for each MCH. There is one MCCH per MBSFN area. Similarly to the MTCH,

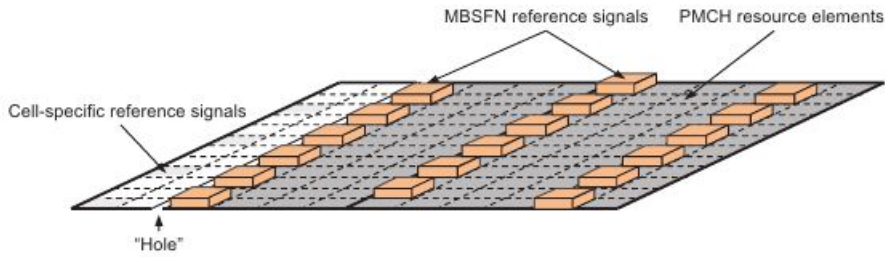


FIGURE 1.4: Resource-block structure and reference-signal structure for MBSFN transmission.

Source: 4G LTE/LTE-Advanced for Mobile Broadband.

the RLC uses unacknowledged mode [1].

In the case of MBSFN-based multicast/broadcast transmission, due to possibly large distances between cells, the cyclic prefix should also cover the timing difference between the transmissions received from the different cells within the MBSFN area. Such timing differences could cause Intersymbol Interference (ISI) which leads to significant performance degradation of the system. Therefore, MCH transmissions use an extended Cyclic Prefix (CP). If a normal CP is used for normal subframes, and therefore also in the control region of MBSFN subframes, there will be a small “hole” between the two parts of an MBSFN subframe, as illustrated in Figure 1.5. This hole is unavoidable if time-synchronization should be applied. The frequency-domain density of MBSFN reference

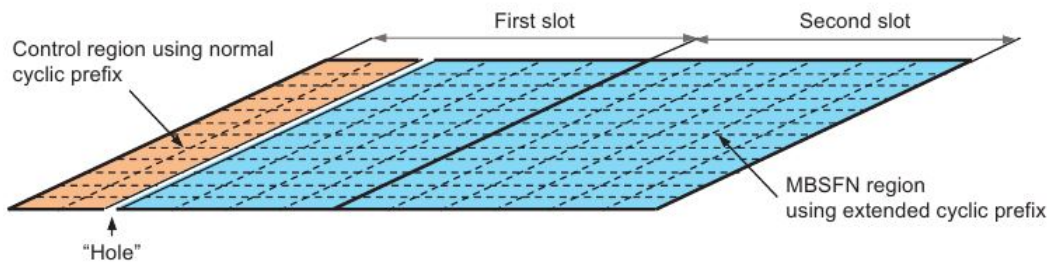


FIGURE 1.5: Resource-block structure for MBSFN subframes, assuming normal cyclic prefix for the control region.

Source: 4G LTE/LTE-Advanced for Mobile Broadband.

symbols is higher than the corresponding density of cell-specific reference symbols. This is important as the total channel of all eNodeBs within the MBSFN area could be treated as a highly time-dispersive or, equivalently, highly frequency-selective. Thus, a higher frequency-domain reference-symbol density for channel estimation is needed.

According to the 3GPPs standard there is only a single MBSFN reference signal in MBSFN subframes. Additionally, multi-antenna transmission is not supported for MBSFN transmission. The main argument for this is that the high frequency selectivity of the aggregated channel itself provides significant frequency diversity. But, as it will be shown in this work, the increase of number of transmit antennas at base station

can substantially increase the overall performance of MBSFN transmission, especially applying some advanced beamforming or precoding techniques.

### 1.3 Road Safety Applications

Road crashes exact a tremendous human and societal casualties in Organisation for Economic Co-operation and Development (OECD) member countries<sup>1</sup>. Each year, more than 125.000 people are killed in such crashes and millions more are injured, many of them permanently. The cost of the road safety problem in the OECD area amounts to 2% or more of gross domestic product [10]. Since the 1970s, as illustrated in Figure 1.6, the amount of road fatalities have declined, which is explained by the intensive collaboration of many countries on the problem of road safety. The key elements of these achievements are safety belts, more safe and secure vehicles, new technologies and systems embedded in passive safety systems and road infrastructure. Improved infrastructure lays the foundation of Intelligent Transportation Systems (ITS).

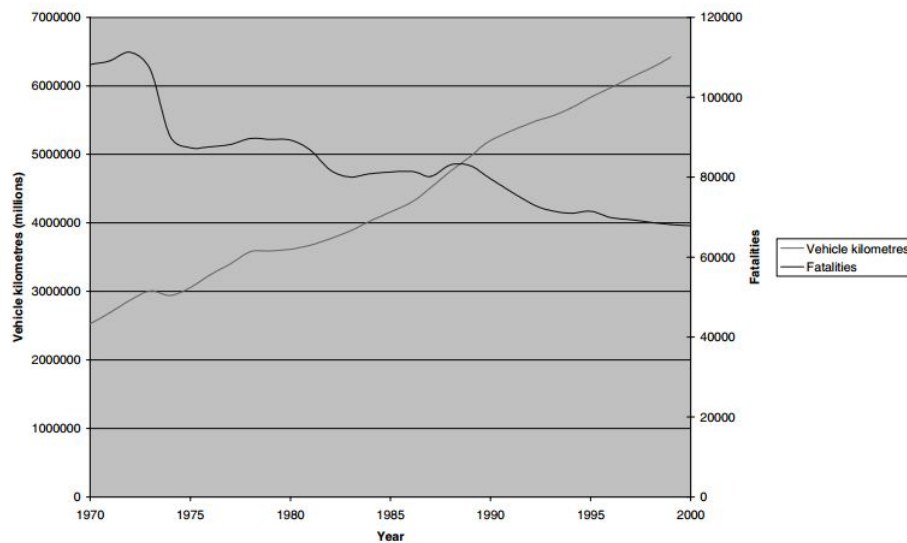


FIGURE 1.6: Road fatalities and vehicle kilometres travelled in nine OECD countries.

*Source:* OECD International Road and Traffic Accident Database.

ITS are advanced applications which aim to provide innovative services relating to different regimes of transport and traffic management. They allow various users to be better informed, more coordinated and to move in safer conditions. In recent years significant amount of additional technologies were included in ITS such as car navigation, traffic signal control systems, weather information, variable message signs, speed cameras to monitor applications and to more advanced applications that integrate live data and

<sup>1</sup>List of OECD members: Austria, Belgium, Canada, Denmark, France, Germany, Greece, Iceland, Ireland, Italy, Luxembourg, The Netherlands, Norway, Portugal, Spain, Sweden, Switzerland, Turkey, United Kingdom, United States.

communicate with different sources, such as parking guidance and information systems. Actually all ITS technologies could be divided into three groups such as autonomous vehicle-based systems, infrastructure-based systems and co-operative systems.

Thereby substantial developments have taken place over the past few years in the area of vehicular communication systems. After the deployment of various vehicular technologies, schematically depicted in Figure 1.7, such as toll collection or active road signs, vehicular communication (VC) systems have emerged. These systems include network nodes which are vehicles and Road-Side infrastructure Units (RSUs) equipped with on-board sensors, processing, and wireless communication modules [11]. Vehicle-to-Infrastructure (V2I), Vehicle-to-Vehicle (V2V) and Vehicle-to-X (V2X) notions emerged. These types of communication allow a range of applications to increase transportation safety and efficiency, as well as video streaming [12]. Especially road safety applications play a very important role in vehicular communications. Road safety applications rely on short-message broadcasting in a vehicle's neighbourhood to inform other vehicles in order to reduce accidents on the road. As a new traffic model, these applications exhibit some unique features in terms of generation patterns and delivery requirements. Particularly, delivery requirements of road safety applications are of high importance, since any signal delay increases the danger of accidents. Two main types of safety messages have been standardized, transmissions of which can be periodic or event-triggered. In European Committee for Standardization (CEN) and European Telecommunications Standards Institute (ETSI) documents [13] these messages are respectively referred to as Cooperative Awareness Messages (CAMs) and Decentralized Environmental Notification Messages (DENMs); Basic Safety Messages (BSMs) are the terminology used in [14] for both periodic and event-triggered messages. CAMs are short messages periodically broadcast from each vehicle to its neighbours to provide information of presence, position, and basic status. DENMs are event-triggered short messages distributed to inform road users of a dangerous event. The main requirements of CAMs and DENMs are reported in Table 1.1, together with the relevant use cases identified by ETSI [15].

In 2013, the ETSI finalized a basic set of standards necessary for the implementation and deployment of cooperative ITS systems, as requested by the European Commission. This set of standards is mainly based on the Institute of Electrical and Electronics Engineers (IEEE) Standards 802.11p [16] access technology for ITS communications, which are defined as ITS G5 communications by the ETSI [17]. The system is well suited to active road safety use cases due to its very low delays and communication range of several hundred meters.

However, the channel congestion experienced in dense scenarios and its decentralized ad-hoc nature is motivating the research of other technologies, such as cellular networks, as alternatives for ITS communications. The latest iteration of 3GPP, known as LTE, promises better levels of quality in terms of throughput and latency compared

TABLE 1.1: Safety message requirements and use cases.

<b>Cooperative awareness message (CAM)</b>	Periodic time-triggered position messages –Frequency: 1–10 Hz –Max latency: 100 ms –Length: up to 800 bytes depending on the type of application	Use cases: –Emergency vehicle warning –Slow vehicle indication –Intersection collision warning –Motorcycle approaching indication –Collision risk warning –Speed limits notification
<b>Decentralized environmental notification message (DENM)</b>	Event-driven hazard warnings –Max latency: 100 ms –Length: typically shorter than CAMs	Use cases: –Emergency electronic brake light –Wrong way driving warning –Stationary vehicle accident –Traffic condition warning –Signal violation warning –Road-work warning –Collision risk warning –Hazardous location –Visibility

with the 3G systems. Nevertheless, it is not clear whether LTE networks can support road safety applications in an effective manner by means of standard unicast transmissions. Similarly to IEEE 802.11p, there is a scalability problem related to the fact that ITS messages have to be delivered to potentially all vehicles in a certain geographical area and with precise delay requirements. If the unicast transmission mode is used, the amount of resources required for the delivery of ITS messages might result in elevated costs for the Mobile Network Operators (MNOs) as well as for the service providers (e.g., car manufacturers). In this context, the utilization of broadcast technologies, such as eMBMS in LTE, appears as a possible solution to solve the scalability problem of ITS in cellular networks. Moreover, there are several additional reasons for LTE applicability in vehicular environments, such as coverage and mobility, market penetration, capacity, centralized architecture, various channels and transport modes as well as different status modes of the terminals. Based on all these arguments, finally, LTE MBSFN can be considered as a potential way to handle vehicular applications.

In the literature, comparing to popular topics from area of mobile communication, investigation of the performance of MBSFNs is not fully investigated, especially in the case of its utilization for road safety applications. Nevertheless there are other studies from neighbour fields, which are focused on the unicast delivery in both 3G [18] and LTE [15] cellular networks. Regarding broadcast delivery, previous studies were only performed in 3G cellular networks [15, 19, 20] without considering new capabilities and solutions introduced by eMBSFN.



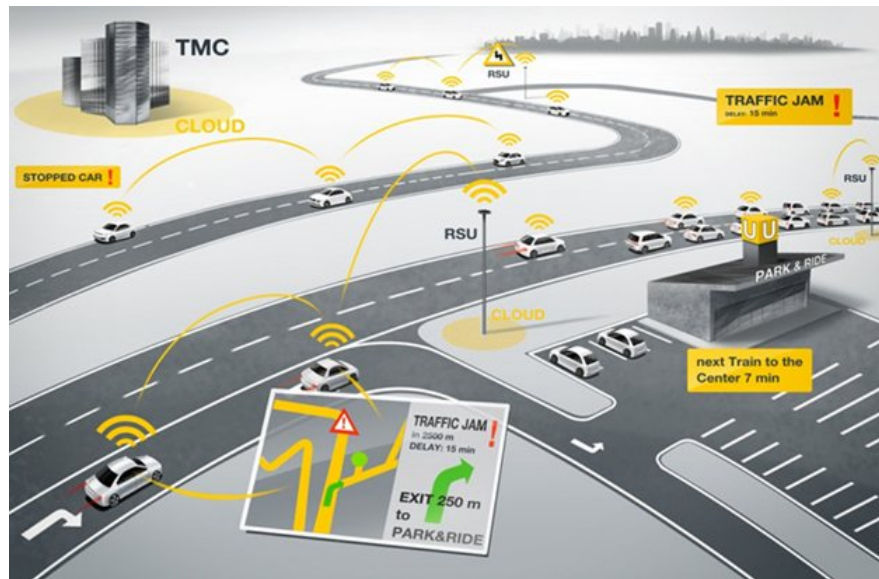


FIGURE 1.7: Illustration of different technologies supporting vehicular communication.  
*Source:*Kapsch

## 1.4 Conclusions

In this chapter a short introduction to LTE MBSFN was done. Especially the architecture, overall channel structure, resource-block structures and downlink channel mapping of MBSFN was explained in more details. A brief explanation of road safety applications, their necessity and importance was stated. Additionally, I explained the main types of road safety messages, their delivery requirements, generation features and relevant use cases. Besides, I considered different possible technologies to handle vehicular communications and provided a short literature research on different solutions. After this investigations, I can claim that LTE could be considered as a possible technology to handle road safety applications, especially in the special case of MBSFN transmission.



## Chapter 2

# Theoretical Basics of OFDM and ICI Modelling

### 2.1 Introduction to Physical layer of LTE

In this section the aspects of physical layer LTE will be considered. Additional consideration of modelling ICI in high mobility scenarios will be performed. To start with basics of OFDM physical layer transmission, at first point explanation of generation of transmitted signal should be performed. The explanation is done in similar way how it is performed in [9].

Let us assume that data symbols  $x_{n,k}; k = 0, 1, \dots, N_c - 1$  should be transmitted over a duration  $T$  at time instant  $n$  and transmit symbol can be expressed as

$$s(t) = \sum_{n=-\infty}^{\infty} \sum_{k=0}^{N_c-1} x_{n,k} g_{T,k}(t - nT), \quad (2.1)$$

Thus, data symbols are modulated with the help of a pulse shaping filter, which has a rectangular shape in time domain

$$g_{T,k}(t) = \begin{cases} \frac{1}{\sqrt{T}} e^{j2\pi k \frac{t}{T}} & 0 \leq t < T \\ 0 & \text{else.} \end{cases} \quad (2.2)$$

For such type of pulse shaping filter, the modulation tends to a so-called OFDM modulation that can be efficiently implemented by a Fast Fourier Transform (FFT). The number of subcarriers  $N_c$  defines the number of individual data streams being transmitted over the wireless channel. Typically the number of subcarriers is equivalent to the order  $N_{FFT} = N_c$  of the FFT operation. One of the important parameters in OFDM modulation is the subcarrier spacing, which can be in this case calculated by dividing the entire transmit bandwidth  $B_c$  by the number of active subcarriers  $N_c$ , thus  $\Delta f = \frac{B_c}{N_c} = \frac{B}{N_{FFT}}$ . However, OFDM modulation theoretically requires an infinite bandwidth due to the

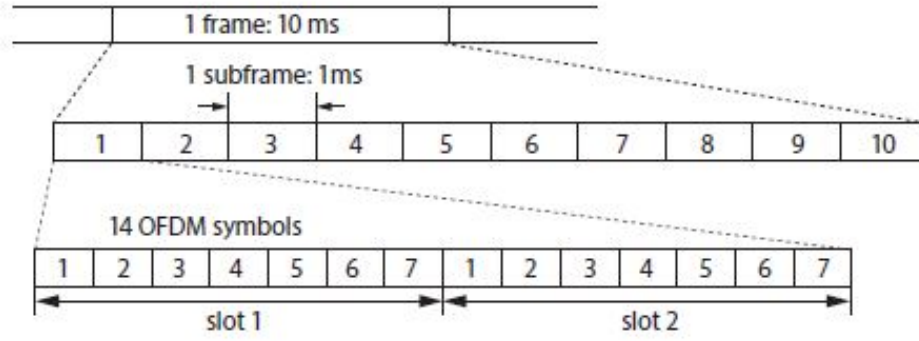


FIGURE 2.1: Frame structure of 3GPP LTE.

unlimited frequency spread of pulse shaping filters in frequency domain. This unlimited spread can be understood from actual calculation of  $g_{T,k}(t)$ :

$$g_{T,k}(t) = g_{T,k}(t) \cdot \text{rect}_T(t). \quad (2.3)$$

Next I assume transmission over a time variant channel. This type of channel is common assumption, especially in the case of highly mobile terminals. The impulse response of such channels can be denoted as  $c(t, \tau)$ . The transmission of generated signal  $s(t)$  over such channel corresponds to convolution in time domain of the signal with the impulse response of the channel. Additionally the signal is corrupted by additive noise, which is usually assumed independent on the channel and transmitted signal. At the receiver antenna the distorted signal can be calculated as

$$r(t) = \int_0^{\tau_{\max}} c(t, \tau) s(t - \tau) d\tau + v(t), \quad (2.4)$$

corrupted by the channel as well as additive noise  $v(t)$ . To avoid distortions caused by a channel with maximal duration  $\tau_{\max}$ , a so-called cyclic prefix is introduced, that is simply a fractional repetition of the transmit signal, placed in front of the signal. Introduction of CP serves two purposes: as a guard interval, it eliminates the ISI from the previous symbol and as a repetition of the end of the symbol, it allows the linear convolution of a frequency-selective multipath channel to be modelled as circular convolution, which in turn may be transformed to the frequency domain using a discrete Fourier transform. Additionally, the last purpose allows for simple frequency-domain processing and representation of the overall transmission system.

In the Downlink (DL) of LTE two possible values of a CP are standardized, a short one of duration  $T_{cp} = 4.7\mu\text{s}$  and a long one of  $T_{cp} = 16.7\mu\text{s}$ . Seven OFDM symbols together with their CP make up one slot ( $N_f = 7$ ). Then the pattern starts again, as is shown in Figure 2.1. The pulse shaping with CP can be best modelled by modifying

the pulse shaping filter to:

$$g_{T_s,k}(t) = \begin{cases} \frac{1}{\sqrt{T}} e^{j2\pi k \frac{t}{T}} & -T_{cp} \leq t < T \\ 0 & \text{else} \end{cases}. \quad (2.5)$$

With such pulse shape, the actual signal duration becomes longer:  $T_s = T + T_{cp}$  which leads to reduced number of time slots in the transmission and as a consequence reduced achievable rates. From the other side this insertion in many cases allows to combat major channel distortions. Applying a rectangular pulse shape and assuming that the channel delays are within  $T_{cp}$  duration, the received signal in (2.4) now can be calculated during the period  $T$  of the OFDM symbol at time instant  $n$  as:

$$r_T(t) = \int_0^{T_s} c(t, \tau) \sum_{k=0}^{N_c-1} x_{nk} g_{T_s,k}(t - \tau - nT_s) d\tau + v(t) \quad (2.6)$$

At the receiver end it is necessary to sample the observed signal. To connect transceiver parameters sampling could be performed with  $N_{FFT}$  samples per period  $T$ . The receiver thus performs at every time instant  $n$  a Fourier transform of the sampled symbol:

$$r_{n,k} = \frac{\sqrt{T}}{N_{FFT}} \sum_{m=0}^{N_{FFT}-1} r_T(t_m = m \frac{T_s}{N_s} + (n-1)T_s + T_{cp}) e^{-j2\pi \frac{mk}{N_{FFT}}} + v_{n,k} \quad (2.7)$$

where  $t_m$  indicates the sampling position within the OFDM symbol.

Now I would like to reformulate this equation in terms of the time-variant transfer function of the channel. The time-variant transfer function of the channel  $C_{t,f}$  can be obtained by applying a Fourier transform with respect to the variable  $\tau$  of the impulse response of the channel. Introduction of the transfer function leads to more simple and clear representation of the received signal, which can now be expressed as:

$$r_{n,k} = \frac{1}{N_{FFT}} \sum_{m=0}^{N_{FFT}-1} \sum_{k'=0}^{N_c-1} C_{m-N_{FFT}+nN_s,k'} x_{n,k'} e^{j2\pi \frac{(k'-k)m}{N_{FFT}}} + v_{n,k}. \quad (2.8)$$

Further work on this equations is needed in order to understand why OFDM transmission could be performed in an efficient way and could be clearly described in terms of simple matrices and vectors.

It is preferable to obtain a simple relationship between transmitted and received data such as  $r_{n,k} = x_{n,k} + v_{n,k}$ , where distortions are caused only by the additive noise term  $v_{n,k}$ . Unfortunately due to the presence of frequency and time variation of the channel there is an additional element, the so called time-variant transfer function  $C_{n,k'}$  of the channel, which depends on the specific subcarrier and time index and as a

consequence the received noisy signal can be expressed as

$$r_{n,k} = \sum_{k'=-1}^{N_c-1} C_{n,k'} x_{n,k'} + v_{n,k} \quad (2.9)$$

Nevertheless, further simplification is possible. In the case, when the subcarrier index of the received signal coincides with the index of the time-invariant transfer function ( $k = k'$  and dependence on time index  $n$  vanish) just one element of transfer function remains and (2.9) collapses to

$$r_{n,k} = C_k x_{n,k} + v_{n,k} \quad (2.10)$$

It means that the time invariant channel matrix collapses just to a single scalar. This allows to reformulate the last expression in terms of matrices and vectors. For example it is possible construct a diagonal channel matrix  $\mathbf{D}$  containing all elements of  $C_k$  on its diagonal. Then it is straightforward to transform the whole transmission model from transmit symbols  $x_{n,k}$  to observed noisy symbols  $r_{n,k}$  after the FFT operation at the receiver in vector notation:

$$\mathbf{r}_n = \mathbf{D}\mathbf{x}_n + \mathbf{v}_n, \quad (2.11)$$

where all data symbols  $x_{n,k}$  at time instant  $n$  over all subcarriers are represented by a single vector  $\mathbf{x}_n \in \mathbb{C}^{N_c \times 1}$  and all values of the sampled received signal  $r_{n,k}$  are included in vector  $\mathbf{r}_n \in \mathbb{C}^{N_c \times 1}$ .

The receiver processing can be reduced to simple matrix multiplication in the case when perfect channel knowledge conditions are fulfilled. Perfect channel knowledge means that at the receiver the full information of  $\mathbf{D}$  is provided. Then it is possible to obtain estimates of  $x_{n,k}$ :

$$\hat{\mathbf{x}}_n = \mathbf{D}^{-1}\mathbf{r}_n = \mathbf{r}_n + \mathbf{D}^{-1}\mathbf{v}_n, \quad (2.12)$$

which is the well-known Zero Forcing (ZF) receiver, specified for SISO transmission.

As soon as the channel is time-variant, however, the situation becomes more complicated. Eq. (2.8) tells now that all data symbols  $x_{n,k}$  at time instant  $n$  of all  $N_c$  subcarriers have an influence on the decoded value. Even in the absence of noise, there exists ICI that corrupts the data and prevents simple detection schemes. It is still possible to describe the connection between  $\mathbf{x}_n$  and  $\mathbf{r}_n$  by a matrix-vector notation. However, matrix  $\mathbf{D}$  is no longer diagonal and also depends on time-instant  $n$ :

$$\mathbf{r}_n = \mathbf{D}_n\mathbf{x}_n + \mathbf{v}_n, \quad (2.13)$$

In particular the elements on the main diagonal  $k = k'$ , are the time-averaged values  $H_{n,k}$  of the channel transfer function  $C_{m,k}$  at time instant  $n$ :

$$H_{n,k} = \frac{1}{N_{FFT}} \sum_{m=0}^{N_{FFT}-1} C_{m-N_{FFT}+nN_s,k} \quad (2.14)$$

With  $\mathbf{h}_n = \text{Diag}(\mathbf{D}_n)$ , it is possible to reformulate Eq. (2.13) in another compact form :

$$\mathbf{r}_n = \text{Diag}(\mathbf{h}_n)\mathbf{x}_n + \mathbf{y}_n^{\text{ICI}} + \mathbf{v}_n, \quad (2.15)$$

where the data is separated into a useful symbol part associated with  $\mathbf{h}_n$  and an interference part  $\mathbf{y}_n^{\text{ICI}}$ , related to off diagonal elements of  $\mathbf{D}$  and data from other subcarriers  $\mathbf{x}_{n,k'}$ . In contrast, for the case of time-invariant channels,  $\mathbf{y}_n^{\text{ICI}}$  is equal to 0. If we know the off-diagonal elements of matrix  $\mathbf{D}$ , then also the part  $\mathbf{y}_n^{\text{ICI}}$  can be considered useful. Nevertheless, in my work I do not consider ICI cancellation techniques.

As shown in Eq. (2.15) the ICI component is relatively complex as it contains data as well as channel components. In literature it is often argued that due to a sum of multiple independent sources, the Central Limit Theorem would hold and the corresponding signal is Gaussian distributed, the nature of this signal is not easily described as such. It certainly can be described by a Gaussian mixture process [21]. Nevertheless, once multiple transmit antennas come into play, ICI can become more Gaussian and with additional coding the obtained ICI impacts throughput of OFDM transmission systems very much like Gaussian distortions with proper signal power. In the next section I will describe how to model ICI in system level simulations. Additionally I will validate obtained results comparing performance with results obtained in Vienna Link Level Simulator[9].

## 2.2 Analytical ICI Model

The goal of this subsection is to explain how to model a fast fading situation by assuming block fading and adding extra ICI noise. In order to describe the impact of ICI some precalculation on the channel should be done. Assume that the impulse response of the channel is described by  $c_{m,m'}$ , where the indices denote the tap gain of the  $m'$ -th tap at time instant  $m$ . I can express  $c_{m,m'}$  as:  $c_{m,m'} = L \cdot \tilde{c}_{m,m'}$ , where  $L$  denotes macroscopic pathloss and shadow fading that remains a constant for a longer time period and  $\tilde{c}_{m,m'}$  represents microscopic fading. I consider for this a so-called Wide-Sense Stationary Uncorrelated Scattering (WSSUS) channel model [22, 23], where the channel can be characterized by its statistics, such as the PDP and its scattering function [23], which is a common assumption in mobile communication. According to these assumptions, and further assuming a two-dimensional propagation scenario, the autocorrelation function

of the channel at time indexes  $m_1, m_2$  and channel taps  $m'_1, m'_2$  can be derived as in [24]:

$$\mathbb{E}\{c_{m_1, m'_1} c_{m_2, m'_2}^*\} = c|L|^2 J_0\left(2\pi f_d T_s (m_1 - m_2)\right) \delta(m'_1 - m'_2), \quad (2.16)$$

where  $c$  is a normalization constant,  $J_0(\cdot)$  denotes the zeroth-order Bessel function of the first kind,  $f_d$  is the Doppler frequency and  $T_s$  is the sampling time. The inverse Fourier transform of the Doppler spectrum is its autocorrelation function which is in two-dimensional propagation scenarios well described by the zeroth-order Bessel function  $J_0(\cdot)$  of the first kind [25]. Additionally, if it is necessary to introduce the impact of transmit power, the Eq. (2.15) can be rewritten as

$$r_{n,k} = H_{n,k} \sqrt{P_{TX}} x_{n,k} + y_{n,k}^{\text{ICI}} + v_{n,k}, \quad k = 0, 1, \dots, N_c. \quad (2.17)$$

where  $P_{TX}$  is transmit power. Introduction of transmit power also impacts the power of ICI. As derived in [26], the power of the ICI term can be calculated as

$$\begin{aligned} \mathbb{E}\{P_{n,k}^{\text{ICI}}\} &= \frac{|L|^2 P_{TX}}{N_{FFT}^2} \sum_{m=0, m \neq k}^{N_c-1} \sum_{m_1=0}^{N_{FFT}-1} \sum_{m_2=0}^{N_{FFT}-1} J_0\left(2\pi f_d \Delta t (m_1 - m_2)\right) \\ &\cdot \exp\left[j \frac{2\pi (m_1 - m_2)(m - k)}{N_{FFT}}\right]. \end{aligned} \quad (2.18)$$

It is now clear that the ICI power is a function of the subcarrier index  $k$ . Further I will indicate the overall ICI power at subcarrier  $k$  as  $P_k^{\text{ICI}} = \mathbb{E}\{|y_{n,k}^{\text{ICI}}|^2\}$ . Obviously here, the averaging has been performed over all possible data and thus the dependency on symbol  $n$  is lost.

### 2.2.1 Extension to MIMO Transmissions

Applying described technique, it is possible to extend ICI modelling to the case of Multiple-Input and Multiple-Output (MIMO) transmission. Let  $\mathbf{F}_k$  be an  $N_T \times N_L$  dimensional semi-unitary precoding matrix. Assuming equal power allocation at transmit antennas (which is consistent with LTE standard) and making an assumption that the channels between the transmit antennas at each base station are statistically independent, it is possible to extend the model as

$$\mathbf{r}_{n,k} = \mathbf{H}_{n,k} \mathbf{F}_{n,k} \mathbf{x}_{n,k} + \mathbf{y}_{n,k}^{\text{ICI}} + \mathbf{v}_{n,k} \quad (2.19)$$

where  $\mathbf{r}_{n,k}$  is the received vector of size  $N_R \times 1$ ,  $\mathbf{H}_{n,k}$  is the averaged channel matrix of size  $N_R \times N_T$ ,  $\mathbf{v}_{n,k}$  is the noise vector and vector  $\mathbf{y}_{n,k}^{\text{ICI}}$  introduces the total ICI power at each time instant  $n$ .



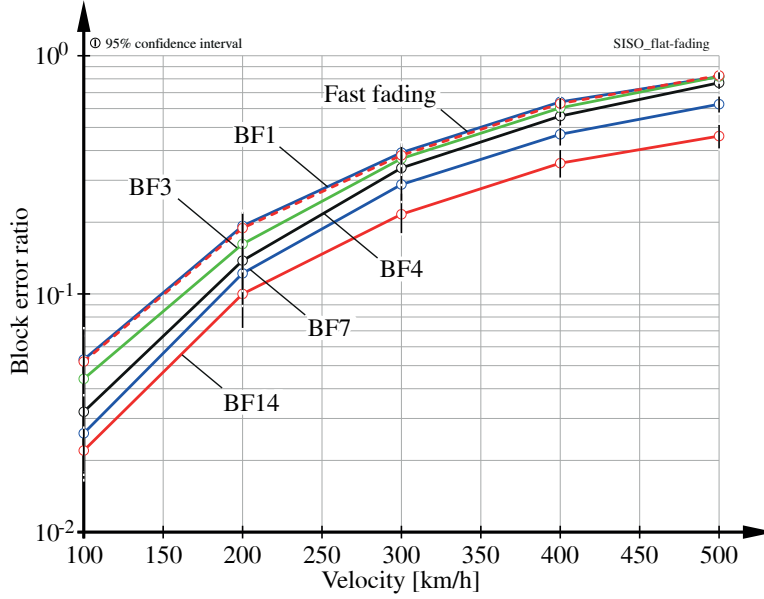


FIGURE 2.2: Comparison of BLER between fast-fading and block-fading simulation with shortened block-fading length. Simulations of block-fading channels with block fading length of 1, 3, 4, 7 and 14 OFDM symbols are considered.

Under an isotropic precoder assumption, the autocorrelation of the transmit signals can be expressed as

$$\mathbb{E}\{(\mathbf{F}_{n,k}\mathbf{x}_{n,k})(\mathbf{F}_{n,k}\mathbf{x}_{n,k})^H\} = \frac{P_{TX}}{N_T}\mathbf{I} \quad (2.20)$$

where  $\mathbb{E}\{\|\mathbf{x}_{n,k}\|_2^2\} = N_L$  and  $\mathbb{E}\{\mathbf{F}_{n,k}\mathbf{F}_{n,k}^H\} = \frac{P_{TX}}{N_T}\mathbf{I}$ . Based on this assumption, the ICI terms from different antennas are uncorrelated. The ICI on receive antenna  $i$ , i.e., element  $[\mathbf{y}_{n,k}^{\text{ICI}}]_i$  of vector  $\mathbf{y}_{n,k}^{\text{ICI}}$ , is obtained by summing up the contributions from all  $N_{TX}$  transmit antennas:

$$[\mathbf{y}_{n,k}^{\text{ICI}}]_i = \sum_{m=1}^{N_{Tx}} y_{n,k}^{\text{ICI},m} \frac{1}{N_T}. \quad (2.21)$$

This finally allows to compute ICI in MIMO transmissions and then add it as additional Gaussian noise in a simple model. Even though the ICI is not Gaussian distributed, it might converge to Gaussian due to central limit theorem for sufficiently large  $N_T$ .

### 2.2.2 Performance Evaluation

In this subsection I provide the validation of my ICI analytical model. The results, which are shown in this subsection, are outcomes from [27]. As already mentioned at the receiver the ICI noise can be approximated as additional complex-valued Gaussian noise with distribution

$$\mathbf{y}_{n,k}^{\text{ICI}} \sim \mathcal{CN}(0, P_{n,k}^{\text{ICI}} \cdot \mathbf{I}). \quad (2.22)$$

To obtain a similar performance to fast fading simulations, however, it is necessary to

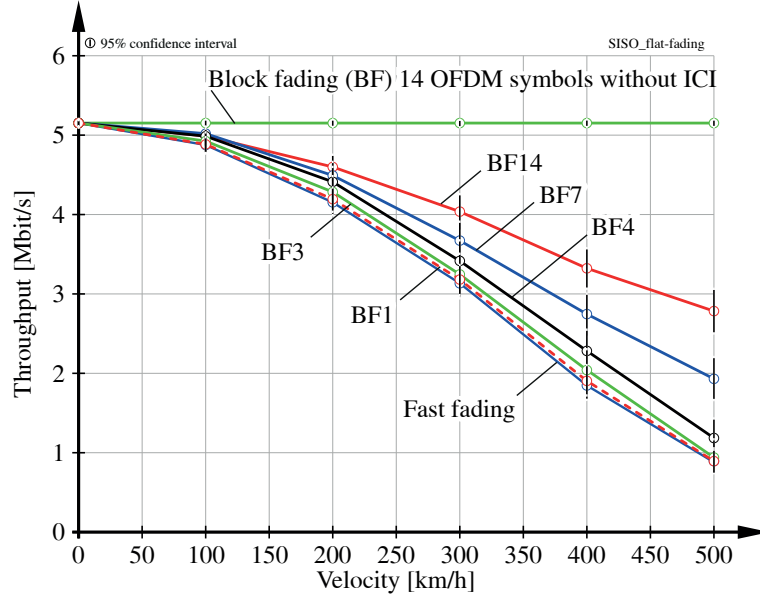


FIGURE 2.3: Justification of ICI abstraction model at 2 GHz center frequency. Simulations of block-fading channels with block fading length of 1, 3, 4, 7 and 14 OFDM symbols are considered.

additionally decrease the length of the fading blocks in case of block fading simulations of high user velocity systems, to account for the reduced coherence time of the channel. Below I demonstrate the validity of the implemented ICI abstraction model by comparing the throughput obtained with fast-fading simulations, i.e., when the channel varies during one OFDM symbol causing ICI, to the performance achieved with block-fading simulations and adding Gaussian noise to emulate the ICI effects. To demonstrate the validity of the implemented ICI abstraction, I compare results with the Vienna LTE Link Level Simulator that allows a very detailed modelling of the various signal sources [9]. In Figure 2.2 and Figure 2.3 I compare the achievable throughput and BLER. Now according to Figures 2.2,2.3, it is clear that adding ICI noise alone is not sufficient. Additionally, shortening the block length improves the accuracy of the model. It is clear that with appropriate ICI calculation and shortened block-fading length it is possible to almost perfectly mimic the fast-fading behaviour and, as a consequence, simulate with high accuracy systems with high mobility users. Similar performance can be observed in the case of MIMO transmissions which is depicted in Figure 2.4 and 2.5, where I compare performance of Vienna LTE Link Level Simulator with fast fading and Vienna LTE System Level Simulator with block fading and extra ICI noise.

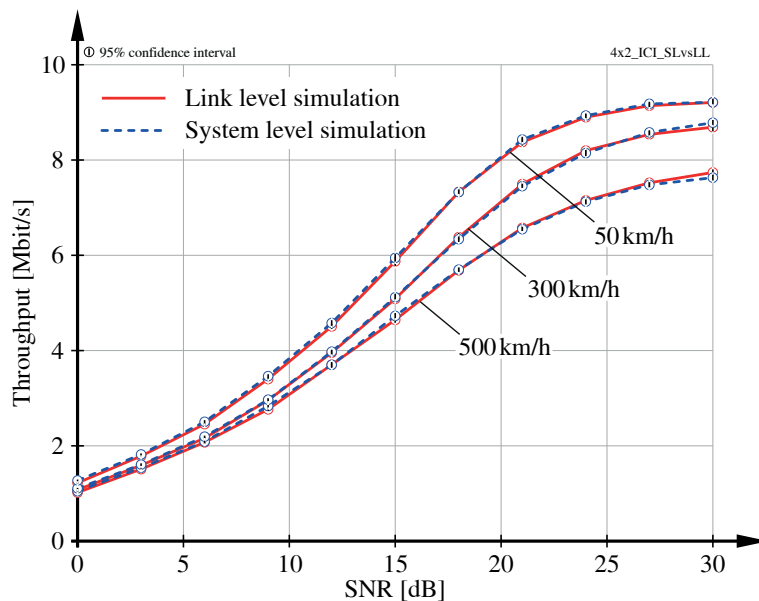


FIGURE 2.4: Comparison of  $4 \times 2$  MIMO transmissions with system and link level simulations.

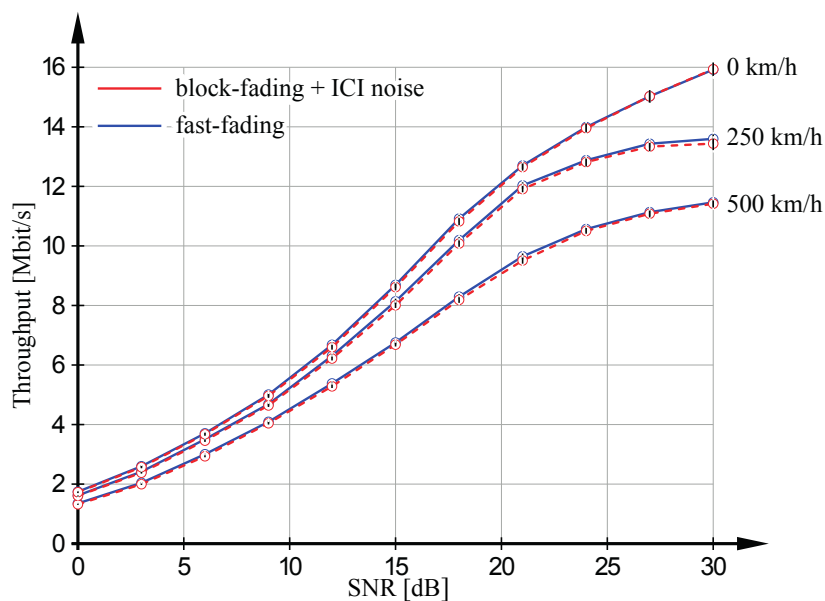


FIGURE 2.5: Comparison of  $4 \times 4$  MIMO transmissions of fast-fading channel and slow fading channel+ ICI noise.

## 2.3 Conclusions

In this chapter I provided description of the physical layer of OFDM, with respect to the LTE specification. I showed that introduction of movement in the system causes significant degradation due to the channel variation within one OFDM symbol. Such variations cause additional distortions, caused by ICI, which plays significant role as soon as I consider highly mobile terminals. In order to simulate such behaviour usually highly

computationally complex fast fading simulations are performed. Due to complexity reasons, fast fading simulations usually are not an option in system level simulators where commonly block fading simulations are preferred. Nevertheless, ICI modeling technique, which was described in this chapter, allows to mimic fast fading behaviour with reasonable complexity. Utilizing this approach I can accurately simulate systems with high mobility users, which helps me further and more precise evaluate performance of LTE MBSFN in the case of road safety applications. Additionally, it should be added, that the complexity of the described technique even for the case of MIMO transmission is comparatively low, which makes this technique even more beneficial.

## Chapter 3

# Physical Layer of LTE MBSFN

### 3.1 System Model

In this chapter I consider the specification of LTE MBSFN transmission from the physical layer point of view. At first I want to introduce the main difference in the input-output relationship between multicast and unicast transmission. Then the main performance metrics will be considered and explained and as well as the ways of their calculation.

At first point I want to consider SISO transmission in the downlink of a cellular network. The transmitter employs OFDM modulation to convert the frequency selective channel into a set of non-interfering frequency-flat subcarriers indexed by  $k$ . The input-output relationship of user  $i$  at subcarrier  $k$  in case of MBSFN transmission is

$$r_{i,k} = \sum_{j \in \text{MBSFN}} h_{i,j,k} \cdot x_{\text{MBSFN},k} + \sum_{l \notin \text{MBSFN}} h_{i,l,k} \cdot x_{l,k} + v_{i,k} \quad (3.1)$$

where  $j$  denotes the base station index in the MBSFN area,  $x_{\text{MBSFN},k}$  denotes MBMS data, which is the same for all multicast users,  $v_{i,k}$  is Additive White Gaussian Noise (AWGN) and  $h_{i,j,k}$  is complex channel coefficient which can be expressed as  $h_{i,j,k} = \gamma_j \cdot \tilde{h}_{i,j,k}$ , where  $\gamma_j$  denotes macroscopic pathloss and shadow fading and  $\tilde{h}_{i,j,k}$  represents microscopic fading.

For standard MBMS transmissions the input-output relationship for user  $i$  can be expressed as

$$r_{i,k} = h_{i,j,k} \cdot x_{\text{MBMS},k} + \sum_{l \neq j} h_{i,l,k} \cdot x_{l,k} + v_{i,k} \quad (3.2)$$

where  $x_{\text{MBMS},k}$  denotes the MBMS data to be transmitted. Based on (3.1) I can express the SINR of multicast user  $i$  in case of MBSFN transmission as

$$\text{SINR}_{i,k,\text{MBSFN}} = \frac{|\sum_{j \in \text{MBSFN}} h_{i,j,k}|^2}{\sigma_v^2 + \sum_{l \notin \text{MBSFN}} |h_{i,l,k}|^2} \cdot \quad (3.3)$$

where the term  $|\sum_{j \in \text{MBSFN}} h_{i,j,k}|^2$  denotes the total power of useful signal received from

all base stations within the MBSFN area, while the term

$\sum_{l \notin \text{MBSFN}} |h_{i,l}|^2$  indicates the power addition of the interference sources. Similarly, based on (3.2) the SINR of MBMS user  $i$  in case of single cell transmission can be expressed as

$$\text{SINR}_{i,k,\text{MBMS}} = \frac{|h_{i,j,k}|^2}{\sigma_z^2 + \sum_{l \neq j} |h_{i,l,k}|^2}. \quad (3.4)$$

Simulation results evaluating the impact of applied channel model can be found in [27].

## 3.2 Multicast Transmit Beamforming

As a more advance technique, which allows to increase the system performance, multicast transmit beamforming could be applied. Multicast transmit beamforming exploits multiple antennas at the transmitter to steer the signal energy towards the served users and to maximize the minimum SINR of multicast users, while constraining the available transmit power. Additionally, as already the max-min SNR beamforming problem for the MISO multicast channel is NP-hard [28], I can conclude that the extension to multiple transmission sources is NP-hard as well.

Assume that I have in total  $J$  base stations within the MBSFN area, each base station serving  $K$  multicast User Equipments (UEs). In the case of road safety applications, multicast UEs denote car users. In order to introduce the impact of beamforming in the case of frequency-flat channel Eq. (3.1) should be rewritten with Multiple-Input Single-Output (MISO) extension as

$$r_i = \sum_{j \in \text{MBSFN}} \mathbf{h}_{i,j}^H \mathbf{f}_j x_{\text{MBSFN}} + \sum_{l \notin \text{MBSFN}} \mathbf{h}_{i,l} \mathbf{x}_l + \mathbf{v}_i \quad (3.5)$$

with  $\mathbf{f}_j \in \mathbb{C}^{N_T \times 1}$  denoting the beamforming vector for base station  $j$  and  $\mathbf{h}_{i,j} \in \mathbb{C}^{N_T \times 1}$  denoting the channel vector from base station  $j$  to user  $i$ . It should be noted that I do not apply any beamforming to base stations which are not within the MBSFN area. The achievable SINR of the multicast user  $i$  from base station  $j$  can be calculated as

$$\text{SINR}_{i,j} = \frac{|\sum_{j \in \text{MBSFN}} \mathbf{h}_{i,j}^H \mathbf{f}_j|^2}{\sigma_n^2 + \frac{1}{N_T} \sum_{l \notin \text{MBSFN}} |\mathbf{h}_{i,l}|^2} \quad (3.6)$$

In the multicast channel the common message is transmitted to all multicast users in parallel. Hence, the multicast transmission rate of the MBSFN area is limited by the minimum of the achievable user rates to ensure error-free reception by all users. The user rate is maximized when the smallest SINR is maximized. I can denote the minimum SINR of the multicast users at base station  $j$  as

$$\text{SINR}_j = \min_{i \in \{1, \dots, K\}} \text{SINR}_{i,j} \quad (3.7)$$

where I simply take the smallest SINR value from the multicast users.

In order to introduce final beamforming problem, some terms require additional explanation. At first point, it should be indicated that joint optimization over all multicast users within MBSFN area is performed. As soon as I have a single optimization problem for multiple base stations I need to introduce general channel vectors, which contain all channels from all base stations within MBSFN area. For example the common channel to user  $i$  will be indicated as  $\mathbf{h}_i \in \mathbb{C}^{N_T \cdot J \times 1}$ . Additionally the beamforming vectors  $\mathbf{f}_j$  are collected into  $\mathbf{f} \in \mathbb{C}^{N_T \cdot J \times 1}$ .

The beamforming problem of maximizing the minimum SINR can be expressed as

$$\max_{\mathbf{F}} \text{SINR} = \max_{\mathbf{F}} \min_{j \in \{1, \dots, J\}} \min_{i \in \{1, \dots, K\}} \text{SINR}_{i,j} \quad (3.8)$$

subject to:

$$\text{trace}(\mathbf{F} \cdot \mathbf{C}_j) \leq P_j, \quad \forall j \in \{1, \dots, J\} \quad (3.9)$$

$$\text{rank}(\mathbf{F}) = 1 \quad (3.10)$$

$$\mathbf{F} \succeq 0 \quad (3.11)$$

where in (3.9)  $P_j$  introduces the power constraint of base station  $j$ , (3.10) is the rank constraint on solution  $\mathbf{F}$ , which is a positive semidefinite transmit covariance matrix  $\mathbf{F} = \mathbf{f}\mathbf{f}^H$  and  $\mathbf{C}_j \in \mathbb{R}^{J \cdot N_t \times J \cdot N_t}$  is the base station dependent power limiting matrix. This matrix has a specific structure: it is a zero matrix, which has ones only on the main diagonal. The amount of these ones and their position depends on the total number of transmit antennas and the total number of base stations within the MBSFN area. For example, if I consider base station 2 and all base stations have 2 transmit antennas and there are 3 base stations in the MBSFN area, then  $\mathbf{C}_2$  will look like

$$\mathbf{C}_2 = \begin{bmatrix} 0 & 0 & 0 & 0 & 0 & 0 \\ 0 & 0 & 0 & 0 & 0 & 0 \\ 0 & 0 & 1 & 0 & 0 & 0 \\ 0 & 0 & 0 & 1 & 0 & 0 \\ 0 & 0 & 0 & 0 & 0 & 0 \\ 0 & 0 & 0 & 0 & 0 & 0 \end{bmatrix} \quad (3.12)$$

Such type of matrix allows to keep individual power constraints in the joint optimization algorithm. Such problems as (3.8) are semidefinite programming problems, which have a non-convex rank constraint and, hence, cannot be solved efficiently [29]. However, I can apply Semidefinite Relaxation (SDR) to the rank constraint to obtain a convex semidefinite program [30]. Introducing a slack variable  $z \in \mathbb{R}$  and defining the global channel Gramian matrices  $\mathbf{R}_i = \mathbf{h}_i \mathbf{h}_i^H$ , it is possible to arrive at the following relaxed

optimization problem:

$$\max_{\mathbf{F} \in \mathbb{C}^{N_T \times J \times N_T}, z \in \mathbb{R}} z \quad (3.13)$$

subject to

$$z \leq \frac{1}{\sigma_{I,n}^2} \text{trace}(\mathbf{R}_i \mathbf{F}), \forall i \in \{1, \dots, K\} \quad (3.14)$$

$$\text{trace}(\mathbf{F} \mathbf{C}_j) \leq P_j, \mathbf{F} \succeq \mathbf{0}, \quad \forall j \in \{1, \dots, J\} \quad (3.15)$$

where  $\sigma_{I,n}^2$  is the sum of noise and interference power.

The problem (3.13) can be solved efficiently by any appropriate solver. In my work I applied CVX in the simulations, a MATLAB-based software package for specifying and solving convex programs [31],[32]. The optimal solution  $\mathbf{F}^*$ , however, is in general not a rank one matrix. Therefore, it is still necessary to convert the optimal solution  $\mathbf{F}^*$  to a feasible solution for  $\mathbf{f}$ .

### 3.2.1 Beamformer Randomization

In this subsection, an approach to transform the optimal solution from problem (3.13) into a feasible and efficient solution of the beamformer  $\mathbf{f}$  is explained. If  $\mathbf{F}^*$  is already a rank-one matrix, the eigendecomposition can be applied to determine the corresponding beamformer. In general, however, it will not output a rank-one matrix; then, randomization is an efficient way to extract a rank-one solution, which, in some cases, provides even provable approximation accuracy with respect to the original (not relaxed) optimization problem [30, 33]. In my work I consider a global randomization method that can be applied by a higher level entity, coordinating the operation of multiple base stations.

Given the optimal transmit covariance matrix  $\mathbf{F}^*$ , the higher level entity, so called coordinator, randomly generates  $N$  candidate beamformer solutions employing Gaussian randomization [30]:

$$\tilde{\mathbf{f}}^n = c_n \phi_n, \quad \phi_n \sim \mathcal{CN}(\mathbf{0}, \mathbf{F}^*), \quad n \in 1, \dots, N \quad (3.16)$$

The normalization constants  $c_n \in \mathbb{R}$  are selected such that the power constraint is not violated.

Finally the coordinator selects the beamformer  $\hat{\mathbf{f}}$  that maximizes the minimum signal power of all multicast users within MBSFN area. The final beamforming vector  $\hat{\mathbf{f}}$ , which contains beamforming vectors for all base stations in MBSFN area, is obtained as

$$\hat{\mathbf{f}} = \arg \max_{n \in \{1, \dots, N\}} \min_{j \in \{1, \dots, J\}} \text{SINR}_j, \quad j \in \{1, \dots, J\} \quad (3.17)$$

The next step is to extract from common beamforming vector  $\hat{\mathbf{f}}$  individual beamformers  $\hat{\mathbf{f}}_j$  and distribute them to the base stations within MBSFN area.



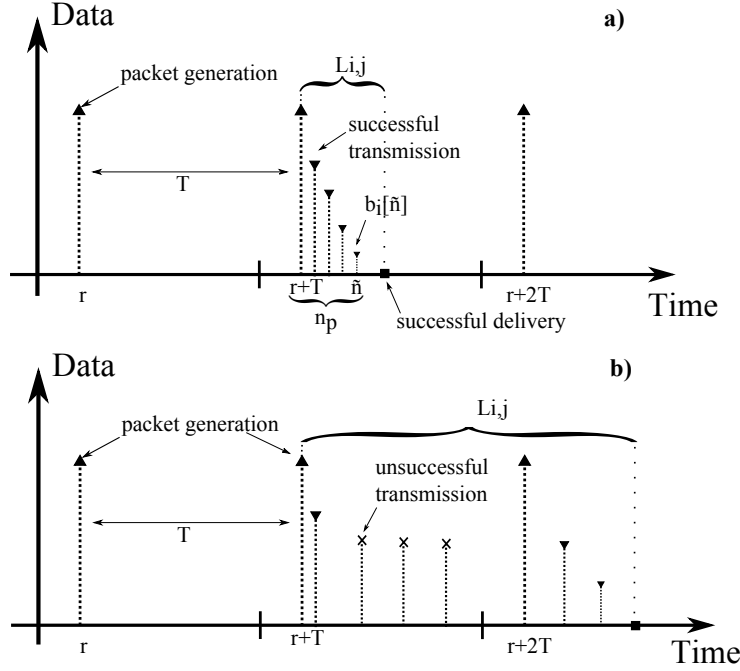


FIGURE 3.1: Explanation of latency calculation.

### 3.3 Performance Metrics

#### 3.3.1 Latency Evaluation

The work [34] is the basis for the outcomes described in this subsection. In my work I assume delay- and error-free uplink transmission from vehicles to base stations and mainly focus on the downlink domain. According to Figure 3.1 I assume that each car user generates MBMS data of size  $p_s$  bits at random starting time  $r$  and then produces packets every  $T$  ms. Such packet generation refers to road-safety applications, when CAMs are generated. These data should be successfully distributed to all other vehicles within the MBSFN area via multicasting. The buffer size of car user  $i$  at time  $\tilde{n}$  can be calculated as

$$b_i[\tilde{n}] = p_s - \sum_{m=1}^{n_p} p_t[\tilde{n} - m] \quad (3.18)$$

where  $p_t[\tilde{n} - m]$  is successfully transmitted packet of size  $p_t$  bits at time  $[\tilde{n} - m]$  and  $n_p$  is specified as

$$n_p = \begin{cases} n - \lfloor \frac{n}{T} \rfloor T - r & , r < \tilde{n}, \quad \tilde{n} = n - \lfloor \frac{n}{T} \rfloor T \\ n - (\lfloor \frac{n}{T} \rfloor - 1)T - r & , r > \tilde{n}, \quad \tilde{n} = n - \lfloor \frac{n}{T} \rfloor T \end{cases} \quad (3.19)$$

which denotes the time difference between packet generation and time instance  $\tilde{n}$ . I consider latency as time interval between data generation and successful delivery to all

appropriate users within the MBSFN area. The latency value can be calculated for both cases of erroneous and error free transmission. According to LTE standard the Hybrid Automatic Repeat Request (HARQ) is not specified in MBMS transmissions. It means that in case of the unsuccessful transmission of a packet, the packet will not be retransmitted but instead I accumulate the latency until I successfully receive the next packet from the same user. Additionally, if during waiting time new packets were generated, the old packets replace them. In Figure 3.1 two cases of latency calculation are shown in more details. In the lower part of Figure 3.1, the latency evaluation in case of successful transmission is described, while in the upper part the procedure of latency accumulation in case of unsuccessful transmission is explained. Assuming a total number of MBMS users equal to  $N_{m\_ue}$  and each of them generating in total  $N_{packets}$  packets, I stack corresponding latency values into a large matrix  $\mathbf{L}$  of size  $N_{packets} \times N_{m\_ue}$ , with elements

$$L_{s,i} = \begin{cases} t_i & , \text{error free transmission} \\ t_i + T \cdot k & , \text{errorneous transmission} \end{cases} \quad (3.20)$$

where  $t_i$  is the time when  $b_i[t_i] = 0$ , i.e. complete transmission of packet  $s$  and  $k$  is the number of required retransmissions. During my investigation I came to the conclusion that the latency evaluation should be performed highly accurately and transparently since interpretation mistake of one of the most important parameters in vehicular communication leads to improper decisions in network specification. Thereby I define three different ways of latency performance indicators:

**Combined latency CDF:** I transform matrix  $\mathbf{L}$  into a vector  $\widehat{\mathbf{L}}$  of size  $N_{packets} \cdot N_{m\_ue} \times 1$  and calculate the empirical cumulative distribution function (ECDF)

$$\text{CDF}_{\text{combined}} = \text{ECDF}(\widehat{\mathbf{L}}) . \quad (3.21)$$

It should be noticed that the main contribution to this latency evaluation is added by the users that have high SINR and, as a consequence, represent significant amount of low latency receptions. Due to relatively big number of small latency, the overall statistic is biased towards small values which, as a consequence, misrepresents final results.

**CDF of mean latency:** I determine the mean latency for each user position (average over all latency values  $s$  obtained at a given user  $i$ ) and calculate the CDF of these mean latencies.

$$\text{CDF}_{\text{mean}} = \text{ECDF}(\widetilde{\mathbf{L}}) \quad (3.22)$$

where  $\widetilde{L}_i = \frac{1}{N_{packets}} \sum_{s=1}^{N_{packets}} L_{s,i}$ . From one side this method allows to avoid an excessive impact presented by previous approach; from the other side it does not represent the worst latencies, which are, however, critical indicators especially for safety-relevant applications (road-safety transmission).

**Latency of individual users:** I determine the latency ECDF of each user position individually, i.e., I obtain  $N_{m\_ue}$  CDFs corresponding to different car users within the network.

### 3.3.2 Network Utilization

Network utilization is considered as another important performance metric which gives better understanding of the price to be paid in terms of throughput of ordinary unicast users for supporting MBSFN transmission. In my investigation I evaluated network utilization as a percentage of resources to be used for sustaining MBMS traffic. It can be calculated as

$$\text{Util} = \frac{p_s \cdot N_{m\_ue}}{N_{RB} \cdot N_{RE} \cdot \text{Efficiency}_{CQI[n]}} \cdot 100\% \quad (3.23)$$

where  $N_{RB}$  is a number of resource blocks,  $N_{RE}$  denotes number of resource elements per resource block and  $\text{Efficiency}_{CQI[n]}$  is the efficiency of the CQI (in bits per resource element) chosen for transmission of MBMS data. With Eq. (3.23) I can calculate the appropriate number of subframes to be reserved for MBMS data transmission, thus satisfying a trade off between MBSFN subframes and subframes used for supporting of ordinary users. The outcome of Eq. (3.23) can be found in Figure 3.2 and Figure 3.3, where I show required number of MBSFN subframes to be reserved for specific CQI value and different number of multicast UEs in the MBSFN area. Additionally this approach helps not to go into network congestions and avoid reservation of excessive number of subframes for MBSFN transmission which is beneficial for the throughput of ordinary unicast users. Network congestion in general meaning indicate the situation when the old message from specific user is not delivered to all MBSFN users while the new message is already generated. This situation has an avalanche effect which leads to significant degradation of the system in terms of latency.

## 3.4 CQI Adaptation

In my work I want to investigate the performance of systems that utilize rate adaptation. Irrespective whether rate adaptation was applied, I reserve the same number of subframes for MBMS data, calculated with Eq.(3.23). However, for rate adaptation the real amount of used subframes could be reduced and unused MBMS subframes can instantaneously be reassigned for ordinary traffic, which may not be feasible in practice. The Channel-Quality Indicators (CQIs) of all users in the MBSFN area are calculated according to the technique proposed in [35] and stored in the vector **CQI**. From the vector **CQI** I choose the smallest CQI index for transmission, in order to support all users. During my research I found that using the smallest CQI index for transmission

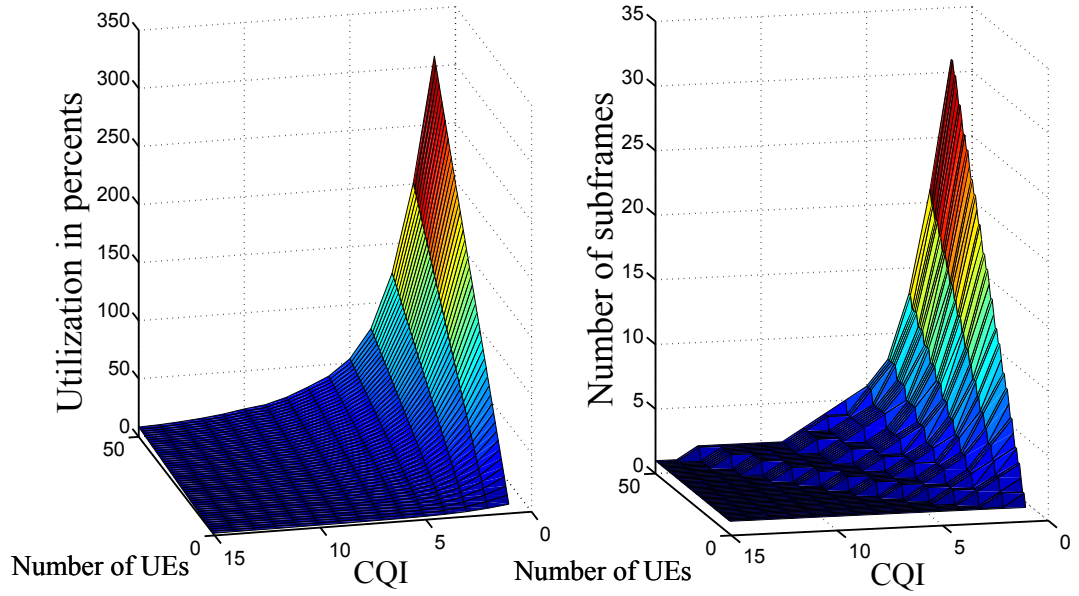


FIGURE 3.2: Utilization of cell resources for different number of UEs.

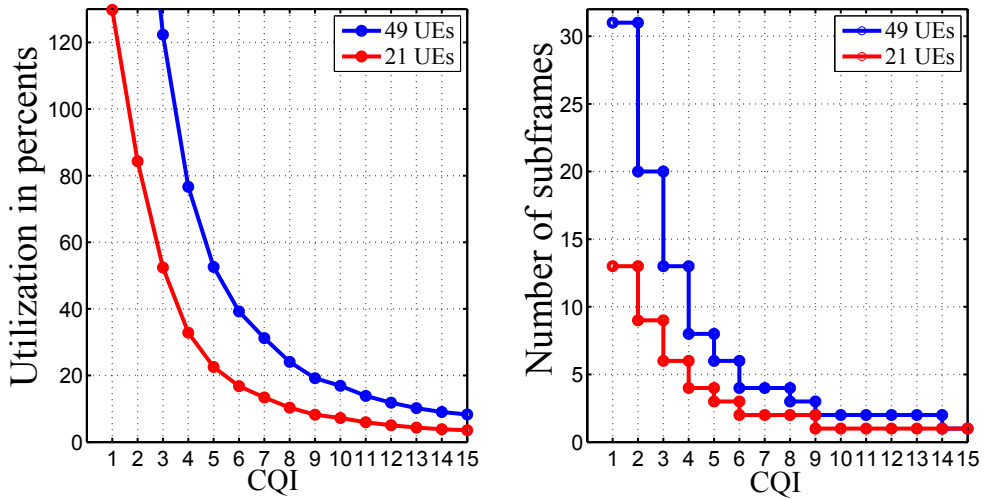


FIGURE 3.3: Comparison of utilization of cell resources for 21 and 49 UEs

can cause traffic congestions (since the number of reserved subframes for MBSFN transmission is too small for supporting communication with such a low efficiency) and I should specify some lower bound ( $CQI_{\text{bound}}$ ) to assure that the generated MBMS traffic can be sustained by the network. Therefore the CQI index at time  $n$  to be used for transmission can be calculated as

$$CQI[n] = \max(\min_i(CQI[i]), CQI_{\text{bound}}) . \quad (3.24)$$

### 3.5 Conclusions

In this Chapter I explained physical layer transmission of LTE MBSFN. I indicated major differences between MBMS and MBSFN transmissions. Additionally an advanced multicast beamforming technique was presented and an efficient suboptimal convex approximation was derived. It should be noted that such types of beamforming techniques usually require full channel knowledge at the transmitter side, which is usually infeasible in real world.

In road safety applications transmission latency is usually considered as one of the most important performance metrics. That is why deep and detailed explanation of latency evaluation was shown. It is remarkable that there are three different types of latencies, all of which have their own advantages and drawbacks. Additionally I explained a mechanism of calculation of network resource utilization, which is another important parameter. The importance of network utilization is explained by the fact that I have standard UEs together with car UEs and I want to handle road safety applications and simultaneously keep the throughput of standard UEs as high as possible. The proposed technique allows me to maintain this trade-off. Finally I explained mechanisms of rate adaptation technique, which I will use in my simulations.



## Chapter 4

# Performance Evaluation

In this chapter I provide a description of the final algorithm that allows to increase the total network performance of MBSFN transmission in the case of its usage in road safety applications. In Chapter 3 physical layer transmission of LTE MBSFN was explained and an efficient multicast beamforming algorithm was presented. This chapter is intended to show how application of the proposed beamforming technique can reduce transmission latency and cell resource utilization in MBSFN systems. Final simulation results will be explained and shown at the end of this chapter.

### 4.1 Description of Simulation Setup

The schematic description of the proposed algorithm can be seen in Algorithm 1. The actual Matlab code for the MBSFN coordinator and CVX solver can be found in Appendix A. The processing chains of the algorithm can be described as follows: through the ideal backhaul MBSFN base stations immediately deliver channel coefficients of all car UEs (obtained from the uplink feedback or other way) to the MBSFN coordinator. At the MBSFN coordinator, calculation of multicast transmit beamforming is performed. This is done via solving the relaxed optimization problems described in Eq. (3.13), then applying beamformer randomization via utilizing Eq. (3.16). According to new SINR values of car UEs, the transmit CQI is determined, applying Eq. (3.24), where  $CQI_{\text{bound}}$  is obtained with Eq. (3.23). The transmit CQI contains information regarding modulation, which should be applied in transmission, together with code rates. After that, eventual beamformers  $\mathbf{f}_j, j \in 1, \dots, J$  with calculated CQI information are delivered back to the base stations. Finally, the MBSFN base stations transmit road safety messages (CAMs), applying beamformers and modulation, obtained from MBSFN coordinator.

```

if support transmit multicast beamforming then
  initialization;
  for All base stations in MBSFN do
    for All car UEs do
      get  $\mathbf{h}_{\text{tot}}$  and  $\mathbf{h}_{\text{int}}$  from the feedback.
       $\mathbf{P}_{\text{int}} = \frac{1}{N_{\text{TX}}}(\mathbf{h}_{\text{int}}\mathbf{h}_{\text{int}}^H)$ ;
       $\mathbf{P}_{\text{n,int}} = \sigma_n^2 + \mathbf{P}_{\text{int}}$ ;
    end
  end
   $\mathbf{F}$  = solve convex problem;
  for All base stations in MBSFN do
    for All car UEs do
       $\text{SINR}_{\text{old}} = \frac{1}{N_{\text{TX}}} \cdot \frac{1}{\mathbf{P}_{\text{n,int}}} \cdot (\mathbf{h}_{\text{tot}}\mathbf{h}_{\text{tot}}^H)$ ;
       $\text{SINR}_{\text{theor}} = \frac{1}{\mathbf{P}_{\text{n,int}}} \cdot \text{trace}(\mathbf{h}_{\text{tot}}\mathbf{h}_{\text{tot}}^H\mathbf{F})$ ;
    end
  end
  randomization;
  choose the best precoders  $\mathbf{f}_j, j \in 1, \dots, J$ ;
  calculate new SINR values;  $\text{SINR} \Rightarrow \text{CQI}$ ;
  CQI adoption:  $\text{CQI}[n] = \max(\min_i(\mathbf{CQI}[i]), \text{CQI}_{\text{bound}})$ 
end

```

**Algorithm 1:** Schematic description of implementation of proposed algorithm.

My simulations were carried out with the Vienna LTE System Level Simulator [36],[37], where I consider an MBSFN area with several high mobility users ("cars") and ordinary unicast users as illustrated in Figure 4.1. Main simulation parameters are listed in Table 4.1. As I explained in previous chapter, car users generate CAMs of size  $p_s = 300$  bytes randomly with interval of  $T$  ms. These messages should be distributed among cars within the MBSFN area. MBMS data should be transmitted in reserved subframes and the standard unicast full buffer users are served with the remaining resources. It should be indicated that for the case of 3 car UEs per base station I reserved 3 subframes within each radio frame for MBMS data and for case of 6 UEs - 5 subframes. These values could be calculated utilizing Eq. (3.23) and applying efficiency corresponding to  $\text{CQI}_{\text{bound}}$ . Additionally, all simulation were done with respect to modelling of ICI, described in Section 2.2.

After this explanation the discussion of the size of the MBSFN area arises. It is clear that with including more and more base stations in the MBSFN area we decrease the number of potential interference sources which leads to improvement of SINR. Nevertheless the large size of the MBSFN area can cause high delay echoes which



TABLE 4.1: Simulation Parameters

<b>Parameter</b>	<b>Value</b>
Center frequency	2.14GHz
System bandwidth	1.4MHz
Channel	Frequency flat fading
Number of b.s. in MBSFN	7
Number of ordinary users per b.s.	1
Number of car users per b.s.	3/6
Speed of car users	100 km/h
Transmission	multicast
Packet size to be transmitted $p_s$	300 bytes
Packet generation interval $T$	100 ms
ICI modelling	Utilized
Transmission rate	Rate adaptation for car users Rate adaptation for ordinary unicast users
Feedback delay	immediate full channel delivery
Antenna configuration	$1 \times 1, 4 \times 1, 8 \times 1$

can further reduce the performance of the system introducing ISI. It should be added that the amount of multicast users will increase with including more base stations and, as a consequence, the amount of generated data will also increase. In the case of common TV broadcasting or any other similar transmission, such effect of data "explosion" will not occur, as the amount of data does not depend on the number of multicast UEs. In contrast, in the case of road safety applications the amount of data is highly dependent on the number of car UEs in the specific area. Thus, high number of car users could cause undesirable congestions in the network and significant delays in transmission due to buffer overflows. Also with increasing the MBSFN area we increase the number of recipients for which the information could be irrelevant. All these circumstances impact the preferred simulation size of the MBSFN area. Applying the network architecture depicted in Figure 4.1, the MBSFN area of seven base stations is surrounded by a ring of interference base stations, which allows to simulate both practical conditions and beneficial features of broadcasting information while avoiding network congestions.

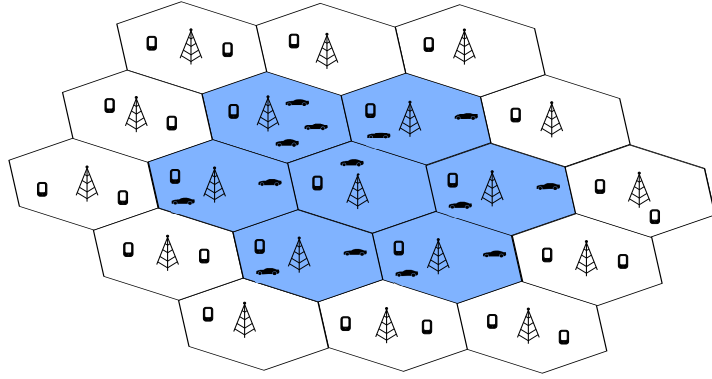


FIGURE 4.1: Illustration of simulated network.

The performance of the baseline scenario is depicted in Figure 4.2. In this and next figures CDFs of mean latency (solid black), combined latency (dashed black) and individual users latency (dotted, color depends on applied beamforming) are presented. These results were obtained with  $1 \times 1$  transmission and applying previously explained CQI adaptation. I want to indicate that the results, which are shown in Figure 4.1 are obtained with transmission, performed according to the LTE standard. According to presented results, the mean transmission latency is 80 ms, which fulfils time constraints required by the standards of CAMs. Nevertheless, the amount of active car UEs in the network is considerably small and the performance can get worse considerably, as soon as the number of car UEs will increase. One possible solution is to increase the number of required MBMS subframes, which will lead to decrease of the latency and to degradation of the achievable throughput of standard unicast UEs. The other solution is to introduce multiple antennas and utilize proposed beamforming technique. Next I want to investigate the impact of MISO transmission and to compare the performance with and without multicast transmit beamforming.

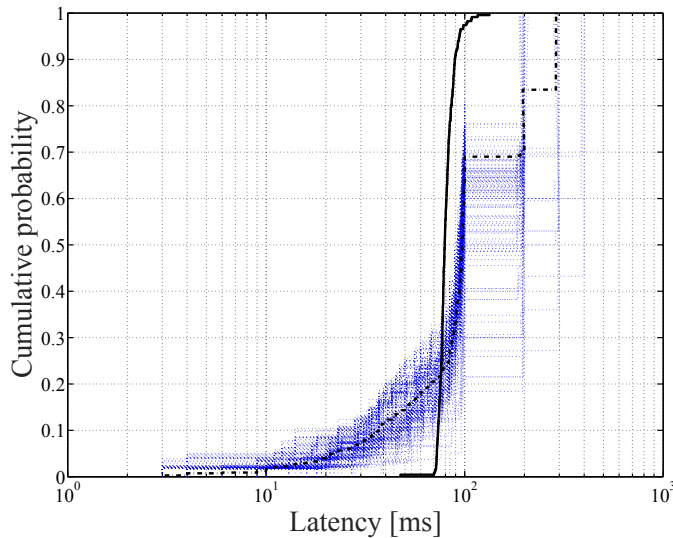


FIGURE 4.2: Latency distribution of baseline scenario with  $1 \times 1$  transmission and 3 car UEs per base station.

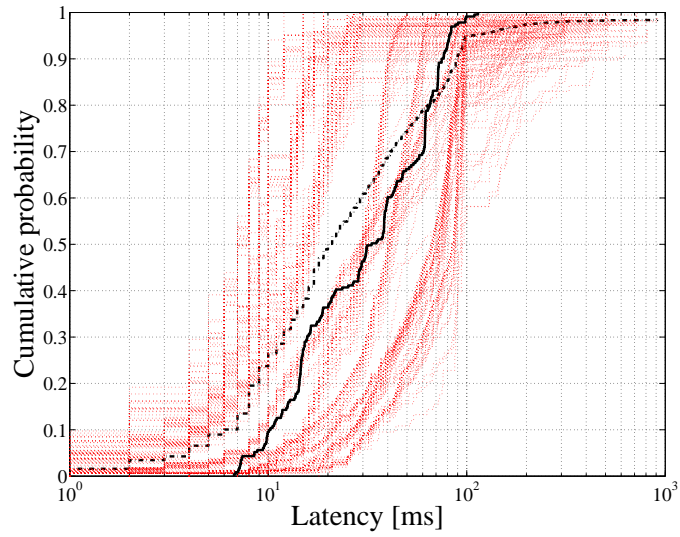
## 4.2 Performance with 4x1 Antenna Configuration

In this section the simulation results with 4 transmit antennas per base station and different number of multicast UEs will be presented. As can be seen in Figure 4.3a extension to MISO without applying any kind of beamforming reduce the mean latency to 33ms. This is achieved due to significant enhancement into SINR of car UEs. Utilization of beamforming technique reduce latency even further, up to 10 ms.

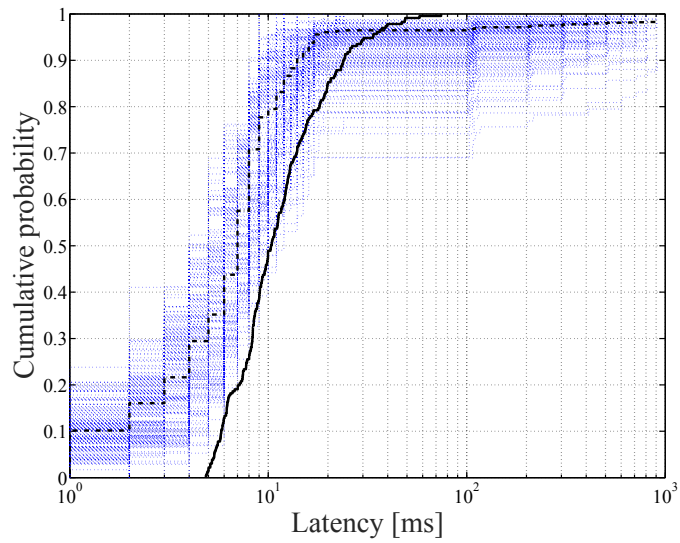
Nevertheless, situation changes dramatically if the number of car UEs is doubled. The latency ecdfs could be seen in Figure 4.4a and Figure 4.4b for the both cases: with and without beamforming. For the case of transmission without beamforming the mean transmission latency is 74 ms. When the number of car UEs per base station is higher then the number of transmit antennas, the performance of beamforming algorithm falls considerably and as a consequence the gain in latency is noticeably reduced: from 74 ms to 70 ms.

In the next step I want to investigate the performance of transmit beamforming algorithm in the case of large number of multicast UEs. I want to explore the impact of beamforming on the SINR distribution of car UEs in the network. Due to complexity reasons I only investigate the case when MBSFN area consist just only of a single base station. In Figure 4.5 the SINR before beamforming, theoretical upper bound and actual SINR distribution are shown. In order to present gains in more transparent way, I collect the smallest values of all three types of SINR (which actually determine the final multicast rate) in Table 4.2. According to results, presented in Table 4.2 I can

state that even in the case of high number of users, proposed algorithm can improve the performance.

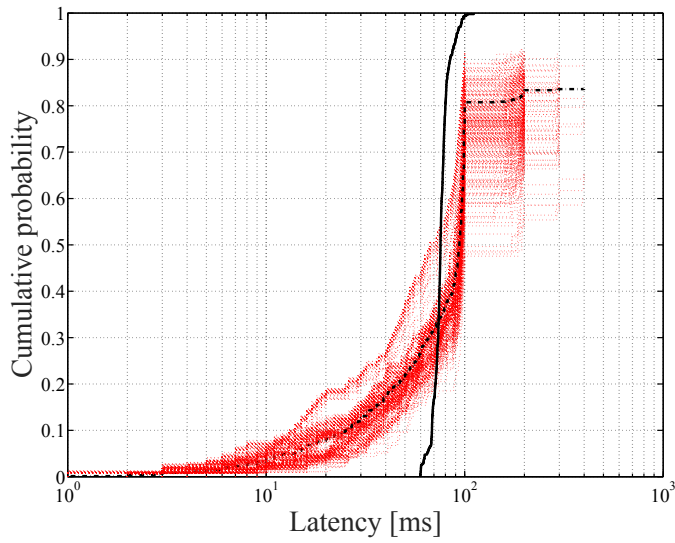


(A) Latency distribution without beamforming.

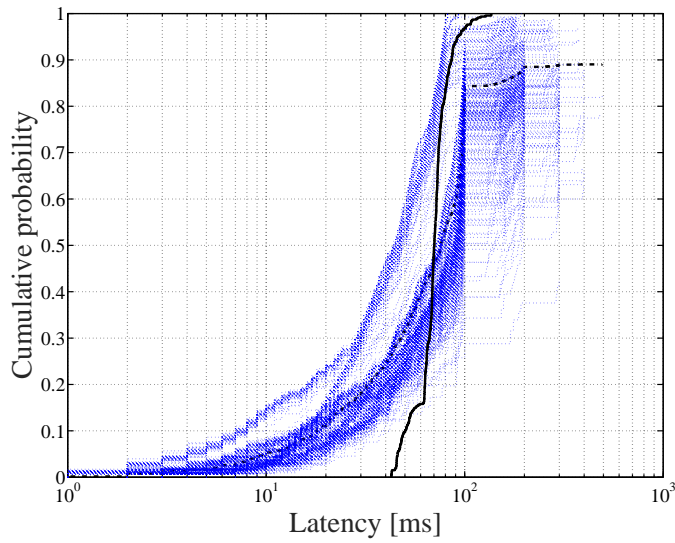


(B) Latency distribution with beamforming.

FIGURE 4.3: Comparison of latency distribution in case of  $4 \times 1$  transmission and total number of 21 multicast UEs in MBSFN area.



(A) Latency distribution transmissions without beamforming.



(B) Latency distribution with beamforming.

 FIGURE 4.4: Comparison of latency distribution in case of  $4 \times 1$  transmission and total number of 42 multicast UEs in MBSFN area.

 TABLE 4.2: Comparison of achievable SINRs with beamforming for  $4 \times 1$  antenna configuration and different number of multicast UEs.

$N_{\text{UEs}}$	$4 \times 1$		
	Old SINR	Actual SINR	Theoretical bound
2	-6.84	-0.82	-0.82
4	-6.46	-1.21	-1.21
8	-10.52	-4.62	-3.2
16	-9.3	-7.53	-4.07
32	-8.71	-7.83	-5.3

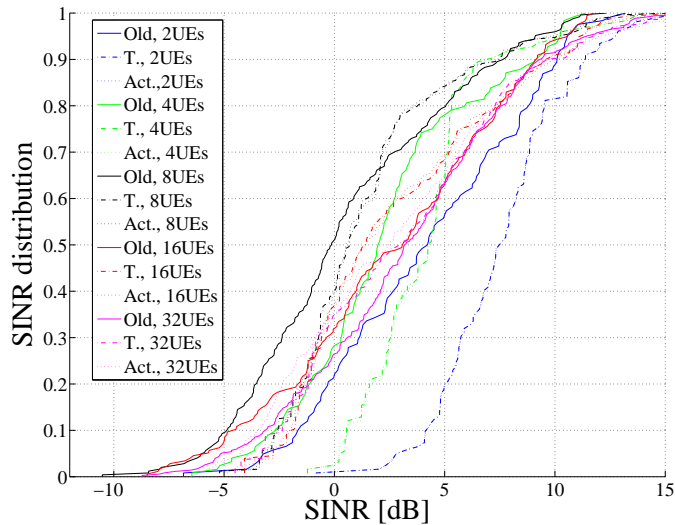


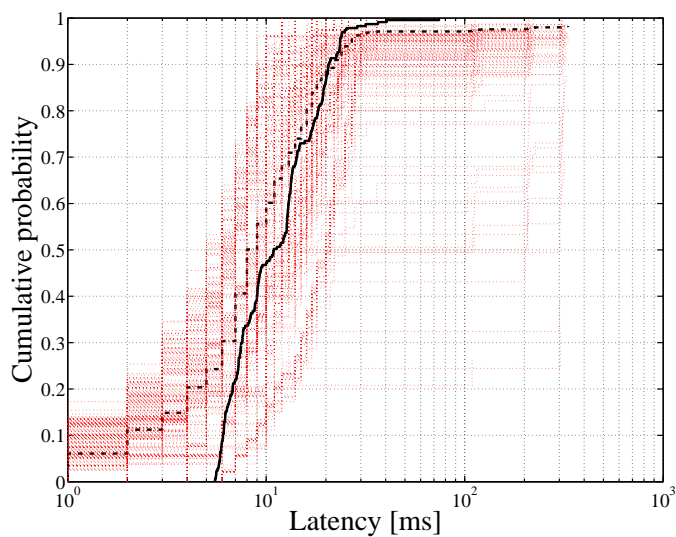
FIGURE 4.5: Comparison of achievable with multicast beamforming SINR values for different number of multicast UEs per base station in case of 4 antennas per base station.

### 4.3 Performance with 8x1 Antenna Configuration

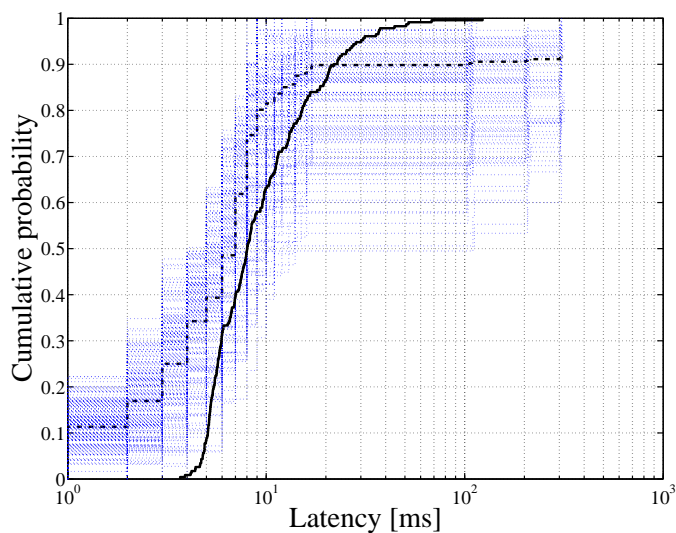
The next step is to show how the performance will behave in the case of 8 transmit antennas per base station. The explanation goes in similar way to the previous section.

As previously, I consider two different number of multicast UEs in the network and performance with and without beamforming. According to Figure 4.6a and Figure 4.6b the performance is even further improved comparing to baseline scenario or scenario with 4 transmit antennas per base station. The mean transmit latency values are 11 ms for the case without beamforming and 8 ms with beamforming. The beamforming gain is not so significant in this case, nevertheless, if situation with 6 car UEs per base station will be considered, the mean latencies will be 54 and 27 ms respectively. Appropriate latency distributions can be found in Figure 4.7a and Figure 4.7b for both cases.

Considering large number of multicast UEs, the beamforming gains are significantly higher, comparing to  $4 \times 1$  case. The SINR distribution and the most important numbers are shown in Figure 4.8 and Table 4.3. It is remarkable, that even in the case of 32 UEs, it is possible to achieve 3dB gain in SINR.



(A) Latency distribution transmissions without beamforming.



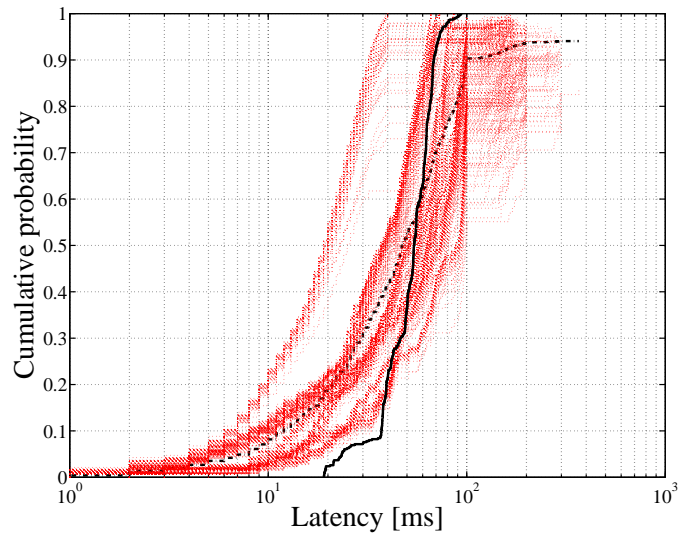
(B) Latency distribution with beamforming.

 FIGURE 4.6: Comparison of latency distribution in case of  $8 \times 1$  transmission and total number of 21 multicast UEs in MBSFN area.

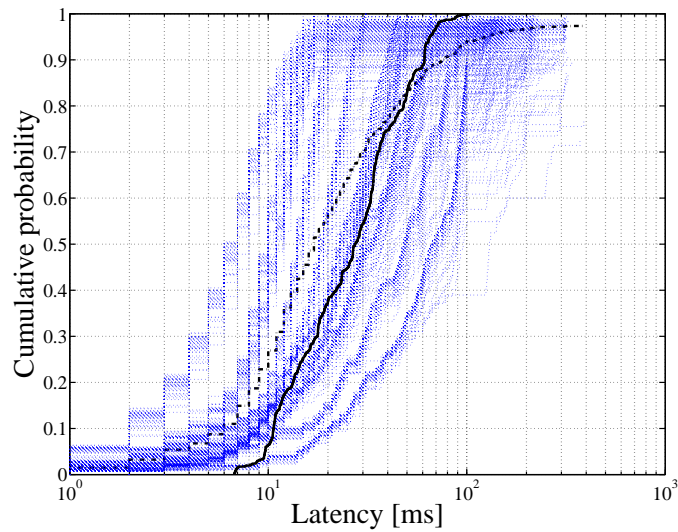
 TABLE 4.3: Comparison of achievable SINRs with beamforming for  $8 \times 1$  antenna configuration and different number of multicast UEs.

$N_{\text{UEs}}$	$8 \times 1$		
	Old SINR	Actual SINR	Theoretical bound
2	-2.78	6.24	6.24
4	-6.12	2.9	2.9
8	-7.53	0.78	0.84
16	-6.37	-0.92	0.76
32	-5.69	-2.13	0.49

H



(A) Latency distribution transmissions without beamforming.



(B) Latency distribution with beamforming.

FIGURE 4.7: Comparison of latency distribution in case of  $8 \times 1$  transmission and total number of 42 multicast UEs in MBSFN area.

## 4.4 Utilization

The question of cell resource utilization will be answered in this section. As mentioned previously, cell resource utilization is another important parameters, especially for MNOs. In Table 4.4 I provide comparison of cell resources consumed by road safety messages. According to presented results, the utilization can be reduced by 33% comparing baseline scenario and  $8 \times 1$  case with beamforming. However, in the dense networks, achievable gains are much smaller and usually in order of 1%.



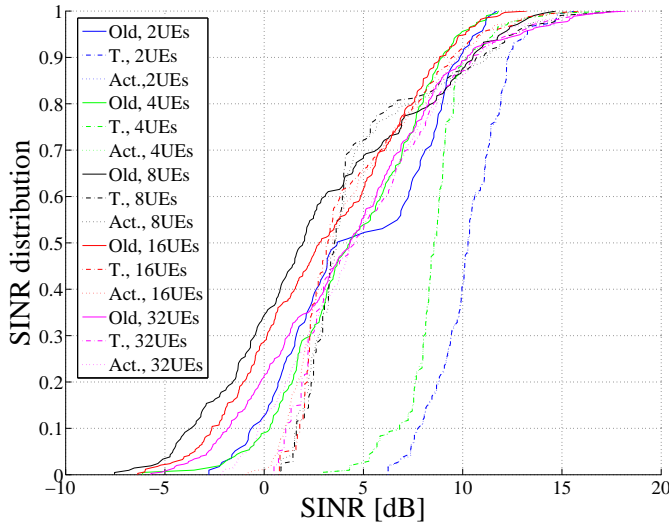


FIGURE 4.8: Comparison of achievable with multicast beamforming SINR values for different number of multicast UEs per base station in case of 8 antennas per base station.

TABLE 4.4: Final comparison of cell resources consumed by road safety messages. Baseline scenario as well as  $4 \times 1$  and  $8 \times 1$  with different number of multicast UEs are considered

	3 car UE	6 car UE
$1 \times 1$	29.75%	-
$4 \times 1$ no beamforming	28%	49.67%
$4 \times 1$ with beamforming	21.94%	49.64%
$8 \times 1$ no beamforming	24.57%	49.57%
$8 \times 1$ with beamforming	20%	48.84%

## 4.5 Conclusions

In this chapter simulation results of the proposed beamforming algorithm in comparison with transmission without beamforming were presented. According to Table 4.5 utilizing beamforming techniques allows to dramatically increase the system performance in terms of latency. Even already the extension to MISO, without max-min beamforming, can improve the situation, especially in the case of small number of multicast UEs in the network. Moreover, the proposed algorithm allows to reduce consumption of cell resources, which is highly preferable for standard unicast UEs.

Additionally in this chapter I showed potential gains for the case of large number of multicast UEs, especially having 8 antennas at the base station I can increase the minimum SINR by a factor of at least 2.27 for the system with 32 multicast UEs

per base station. And this gain could be increased even further if more and more base stations will be included in the MBSFN area.

TABLE 4.5: Final comparison of mean transmission latency between performance of standard LTE MBSFN transmission and more advanced approaches for different number of car UEs in the network.

	3 car UE	6 car UE
$1 \times 1$	80 ms	-
$4 \times 1$ no beamforming	33 ms	74 ms
$4 \times 1$ with beamforming	10 ms	70 ms
$8 \times 1$ no beamforming	11 ms	54 ms
$8 \times 1$ with beamforming	8 ms	27 ms

## Chapter 5

# Conclusions

In this work, the performance of MBSFN transmission in connection with road safety applications was investigated. As additional tools which allow to increase preciseness of simulations and to enhance the performance of the system, ICI modelling and transmit beamforming techniques were introduced.

In Chapter 1 a short introduction to the architecture of MBSFN area was presented, as well as a brief explanation of vehicular communication, specifically road safety application, was provided. Due to advanced broadcast/multicast capabilities introduced by MBSFN, possibility to support road safety application through cellular networks emerged. From the road safety messages point of view, due to their specific generation and delivery peculiarities, MBSFN transmission could be seen as one of the most promising candidate.

As preliminary investigation, technique for modelling ICI effects was introduced in Chapter 2. ICI presence is a result of time-varying nature of the wireless channels, especially in systems with high mobility terminals. Due to severe effects on the performance, ICI should be precisely modelled and accounted in such systems. Nevertheless, direct calculation of ICI requires utilization of computationally complex fast-fading simulations, which are usually not an option in system level simulations. However, according to the results represented in Chapter 2 of this work, ICI can be modelled as additional coloured Gaussian noise which can be added at the receiver. Moreover, this approach does not introduce any significant complexity problems, which allows to use it efficiently in my simulations.

In Chapter 3 I presented basics of MBSFN physical layer transmission where I showed the advantage of MBSFN versus MBMS in terms of SINR. Additionally I introduced several concepts of transmission latency evaluation. I should point out one important consequence: the full picture of packet delivery latency is only provided if I do not apply any kind of latency aggregation over users and/or time. As a helpful tool, I showed how precalculation of expected amount of resource consumptions allows

to avoid traffic congestions for multicast UEs and simultaneously to retain throughput of ordinary UEs as high as possible.

Introduction of multiple antennas at base stations permits to utilize different beamforming technique. One probable beamforming approach was presented in Chapter 3. The idea of this approach is to increase the minimal SINR value of multicast users in order to increase the multicast transmission rates. It should be noted that this algorithm introduces some new features, such as joint optimization over multiple base stations with individual power constraints. Additionally, through the particularity of multicasting, where the signals from multiple base stations are treated as useful, from the point of view of the users, joint optimization could be treated as optimization over one base station with huge amount of antennas. This interpretation allows potentially to have tremendous gains, especially for the small amount of multicast users.

Due to their non-convex nature it is not always possible to obtain optimal solution for beamforming optimization problems. However, via utilization of randomization, it is possible in some cases to obtain provable approximation accuracy with respect to the theoretical upper bound. To the drawbacks of proposed beamforming technique I can attribute a high sensitivity to the feedback delay and obligatoriness of the perfect channel knowledge. In my work I always assumed instantaneous channel knowledge at the MBSFN coordinator which is not feasible in real world circumstances. For real world scenarios, the proposed technique requires an additional extension. All my simulations were performed with 1.4 MHz transmission bandwidth, which means optimization was done over six resource blocks. The utilization of a bigger bandwidth could increase the computational demand to an infeasible level in real life application, which could be pointed as another drawback. One possible way to improve the robustness to channel variations is to perform transmissions with CQI values smaller than those obtained with Eq. (3.24).

Chapter 4 showed that the extension of the LTE MBSFN standard to multiple antennas in itself brings alone significant improvements. As was shown in Table 4.5 and Table 4.4 the employment of the proposed algorithm allows to reduce transmission latency by a factor of 10 and resource utilization by 33% comparing to the baseline scenario.

# Appendix A

## Detailed description of the applied algorithm

LISTING 1: Actual Matlab code for the transmit multicast beamforming calculation.

---

```
1 NU = length(UEs)/length(obj.MBSFN_area_eNodeBs);
2 TX = obj.MBSFN_area_eNodeBs(1).nTX;
3 NB = length(obj.MBSFN_area_eNodeBs);
4 H_tot = zeros(TX*NB,NU,NB);
5 H_int_tot = zeros(TX,TX,NU);
6 noise_and_int = zeros(1,NU,length(obj.MBSFN_area_eNodeBs));
7 bb_ind = false(TX*NB,NB);
8 bb_l = false(TX*NB,NB);
9 for bb = 1:NB
10     if size(H_tot,1)/length(obj.MBSFN_area_eNodeBs) == 4
11         bb_ind(bb*TX-3:bb*TX,bb) = true;
12     else
13         bb_ind(bb*TX-7:bb*TX,bb) = true;
14     end
15     bb_l(:,bb) = ~bb_ind(:,bb);
16     for u_i = 1:NU
17         H_tot(bb_ind(:,bb),u_i,bb) = ...
18             squeeze(obj.MBSFN_area_eNodeBs(bb).attached_UEs_vector(u_i).feedback.H_0(:,:,1));
19         h_i_temp = ...
20             obj.MBSFN_area_eNodeBs(bb).attached_UEs_vector(u_i).feedback.H_i(:,:,1,1,:);
21         int_power = 1/TX*(h_i_temp(:,:)*h_i_temp(:,:))';
22         noise_var_temp = ...
23             obj.MBSFN_area_eNodeBs(bb).attached_UEs_vector(u_i).thermal_noise_W_RB;
24         noise_and_int(:,u_i,bb) = noise_var_temp+trace(int_power);
25     end
26 end
27 %calling optimizer
28 F = network_elements.max_min_precoder_MBSFN_interf(H_tot,TX,NB,NU,noise_and_int);
29 for bb=1:NB
30     for u_i = 1:NU
31         SINR_theoretical_new(u_i,bb) = ...
```

```

32         (1/noise_and_int(:,u_i,bb))*trace(H_tot(:,u_i,bb)*H_tot(:,u_i,bb)'+F);
33     SINR_old(u_i,bb) = ...
34         (1/TX)*(1/noise_and_int(:,u_i,bb))*trace(H_tot(:,u_i,bb)*H_tot(:,u_i,bb)');
35     end
36 end
37 [U,S,V] = svd(F);
38 %% Randomization part
39 fi_tot = zeros(size(F,1),500);
40 sqrtF = U*sqrt(S)*V';
41 for prec_ind = 1:500
42     fi_tot(:,prec_ind) = ...
43         sqrtF*1/sqrt(2)*(randn(size(F,1),1)+1i*randn(size(F,1),1));
44     %renormalization
45     for i = 1:NB
46         fi_tot_mat(:,i) = fi_tot(i*TX-TX+1:i*TX,prec_ind);
47         norm_fi(i) = norm(fi_tot_mat(:,i));
48     end
49     [max_norm,ind] = max(norm_fi);
50     fi_tot(:,prec_ind) = fi_tot(:,prec_ind)/max_norm;
51     %finding the smallest SINR
52     for i = 1:NB
53         for u_i = 1:NU
54             SINR_temp(u_i,i) = ...
55                 (1/noise_and_int(:,u_i,i))*abs(H_tot(:,u_i,i)'+fi_tot(:,prec_ind))^2;
56         end
57     end
58     SINR_min(prec_ind) = min(min(SINR_temp));
59 end
60
61 [var,prec_index] = max(SINR_min);
62
63 for i = 1:length(obj.MBSFN_area_eNodeBs)
64     for u_i = 1:NU
65         SINR_new(u_i,i) = ...
66             (1/noise_and_int(:,u_i,i))*abs(H_tot(:,u_i,i)'+fi_tot(:,prec_index))^2;
67     end
68 end

```

---

LISTING 2: Matlab code for CVX solver.

---

```

1 function F = max_min_precoder_MBSFN_interf(h_full_bar,Tx,Nb,UU,noise_and_int)
2
3     cvx_begin quiet
4     variable F(Nb*Tx,Nb*Tx) complex semidefinite
5     variable z
6     maximize z;
7     subject to
8         C = zeros(Nb*Tx,Nb*Tx,Nb);
9         for i = 1:Nb
10            A = zeros(1,Nb*Tx);

```

```
11         A(Tx*i-(Tx-1):Tx*i) = 1;
12         C(:, :, i) = diag(A);
13         trace(F*C(:, :, i)) <= 1;
14     end
15     for bb = 1:Nb
16         for uu = 1:UU % channel gain
17             z <= trace(F*h_full_bar(:, uu, bb)*h_full_bar(:, uu, bb)')/noise_and_int(:, uu, bb);
18         end
19     end
20     cvx_end
21 end
```

---





# Bibliography

- [1] Erik Dahlman, Stefan Parkvall, and Johan Skold. *4G: LTE/LTE-Advanced for Mobile Broadband*. Academic Press, 1st edition, 2011. ISBN 012385489X, 9780123854896.
- [2] 3GPP. TSG RAN; introduction of the multimedia broadcast multicast service (mbms) in the radio access network (ran); stage 2 (release 6). <http://www.3gpp.org/DynaReport/25346.htm>, Sept. 2006.
- [3] Ericsson. LTE broadcast: a revenue enabler in the mobile media era, Feb. 2013. White paper.
- [4] Valter D’Avino (Ericsson). Ericsson and Polkomtel test LTE broadcast in Poland, Sept. 1. 2014. Press release.
- [5] Deby Lewis (Verizon). Verizon delivers LTE multicast over commercial 4G LTE network in Indy, May 21. 2014. Press release.
- [6] Bill Smith (AT&T). AT&T LTE broadcast demo at college football national championship showcases exciting network future, Jan. 16. 2015. Press release.
- [7] T. Lohmar, M. Slsingar, S. Puustinen, and V. Kenehan. Delivering content with LTE broadcast. *Ericsson review: the communications technology journal since 1924*, 2013(1), Feb. 2013.
- [8] D. Valerio, F. Ricciato, P. Belanovic, and T. Zemen. UMTS on the Road: Broadcasting Intelligent Road Safety Information via MBMS. In *67th IEEE Vehicular Technology Conference (VTC2008-Spring)*, pages 3026–3030, Singapore, May 2008.
- [9] Markus Rupp, Stefan Schwarz, and Martin Taranetz. *The Vienna LTE-Advanced Simulators: Up and Downlink, Link and System Level Simulation*. Signals and Communication Technology. Springer Singapore, 1 edition, 2016. ISBN 978-981-10-0616-6. doi: 10.1007/978-981-10-0617-3.
- [10] OECD reports. Road safety impact of new technologies. 2003.

- [11] Panagiotis Papadimitratos, Levente Buttyan, Tamás Holczer, Elmar Schoch, Julien Freudiger, Maxim Raya, Zhendong Ma, Frank Kargl, Antonio Kung, and J-P Hubaux. Secure vehicular communication systems: design and architecture. *Communications Magazine, IEEE*, 46(11):100–109, 2008.
- [12] J. Calabuig, J.F. Monserrat, D. Gozalvez, and O. Klemp. Safety on the roads: LTE alternatives for sending ITS messages. *Vehicular Technology Magazine, IEEE*, 9(4): 61–70, Dec 2014.
- [13] ETSI EN ETSI. 302 665 v1. 1.1: Intelligent transport systems (ITS), Communications Architecture. *European Standard (Telecommunications Series)*, Sept. 2010.
- [14] RITA. Intelligent Transportation Systems Joint Program Office. Core System Concept of Operations (ConOps). October 2011.
- [15] G. Araniti, C. Campolo, M. Condoluci, A. Iera, and A. Molinaro. Lte for vehicular networking: a survey. *IEEE Communications Magazine*, 51(5):148–157, May 2013. ISSN 0163-6804. doi: 10.1109/MCOM.2013.6515060.
- [16] IEEE 1609 - Family of Standards for Wireless Access in Vehicular Environments (WAVE), April 13 2013.
- [17] D. Jiang and L. Delgrossi. Ieee 802.11p: Towards an international standard for wireless access in vehicular environments. In *Vehicular Technology Conference, 2008. VTC Spring 2008. IEEE*, pages 2036–2040, May 2008. doi: 10.1109/VETECS.2008.458.
- [18] T. Mangel and H. Hartenstein. An analysis of data traffic in cellular networks caused by inter-vehicle communication at intersections. In *Intelligent Vehicles Symposium (IV), 2011 IEEE*, pages 473–478, June 2011. doi: 10.1109/IVS.2011.5940495.
- [19] D. Valerio, F. Ricciato, P. Belanovic, and T. Zemen. UMTS on the Road: Broadcasting Intelligent Road Safety Information via MBMS. In *Vehicular Technology Conference, 2008. VTC Spring 2008. IEEE*, pages 3026–3030, May 2008. doi: 10.1109/VETECS.2008.325.
- [20] M. Wetterwald. A case for using mbms in geographical networking. In *Intelligent Transport Systems Telecommunications, (ITST), 2009 9th International Conference on*, pages 309–313, Oct 2009. doi: 10.1109/ITST.2009.5399336.
- [21] Tiejun Wang, J. G. Proakis, E. Masry, and J. R. Zeidler. Performance degradation of ofdm systems due to doppler spreading. *IEEE Transactions on Wireless Communications*, 5(6):1422–1432, June 2006. ISSN 1536-1276. doi: 10.1109/TWC.2006.1638663.

- [22] Philip Bello. Characterization of randomly time-variant linear channels. *IEEE Transactions on Communications Systems*, 11(4):360–393, 1963.
- [23] Andreas Molisch. *Wireless Communications*. Wiley-IEEE Press, 2005. ISBN 047084888X.
- [24] Yang-Seok Choi, Peter J Voltz, and Frank A Cassara. On channel estimation and detection for multicarrier signals in fast and selective Rayleigh fading channels. *IEEE Transactions on Communications*, 49(8):1375–1387, 2001.
- [25] RH Clarke. A statistical theory of mobile-radio reception. *Bell system technical journal*, 47(6):957–1000, 1968.
- [26] Yang-Seok Choi, Peter J Voltz, and Frank A Cassara. On channel estimation and detection for multicarrier signals in fast and selective Rayleigh fading channels. *IEEE Transactions on Communications*, 49(8):1375–1387, 2001.
- [27] I. Safiulin, S. Schwarz, and M. Rupp. System level simulation of LTE MB-SFN networks with high mobility users. In *Systems, Signals and Image Processing (IWSSIP), 2015 International Conference on*, pages 21–24, Sept 2015. doi: 10.1109/IWSSIP.2015.7313927.
- [28] N. D. Sidiropoulos, T. N. Davidson, and Zhi-Quan Luo. Transmit beamforming for physical-layer multicasting. *IEEE Transactions on Signal Processing*, 54(6): 2239–2251, June 2006. ISSN 1053-587X. doi: 10.1109/TSP.2006.872578.
- [29] A. B. Gershman, N. D. Sidiropoulos, S. Shahbazpanahi, M. Bengtsson, and B. Ottersten. Convex optimization-based beamforming. *IEEE Signal Processing Magazine*, 27(3):62–75, May 2010. ISSN 1053-5888. doi: 10.1109/MSP.2010.936015.
- [30] Z. q. Luo, W. k. Ma, A. M. c. So, Y. Ye, and S. Zhang. Semidefinite relaxation of quadratic optimization problems. *IEEE Signal Processing Magazine*, 27(3):20–34, May 2010. ISSN 1053-5888. doi: 10.1109/MSP.2010.936019.
- [31] M. Grant and S. Boyd. *CVX: Matlab software for disciplined convex programming, version 2.1*, March 2014. URL <http://cvxr.com/cvx>.
- [32] V. Blondel, S. Boyd, and H. Kimura. *Graph implementations for nonsmooth convex programs*, 2008.
- [33] S. Schwarz. Probabilistic analysis of semidefinite relaxation for leakage-based multicasting. *IEEE Signal Processing Letters*, 23(5):742–746, May 2016. ISSN 1070-9908. doi: 10.1109/LSP.2016.2550618.

- [34] Illia Safiulin, Stefan Schwarz, Tal Filosof, and Markus Rupp. Latency and resource utilization analysis for V2X communication over LTE MBSFN transmission. arXiv:1510.06547, 2015.
- [35] Stefan Schwarz and Markus Rupp. Throughput maximizing feedback for MIMO OFDM based wireless communication systems. In *The 12th IEEE International Workshop on Signal Processing Advances in Wireless Communications (SPAWC)*, pages 316–320, 2011.
- [36] Stefan Schwarz, Josep Colom Ikuno, Michal Simko, Martin Taranetz, Qi Wang, and Markus Rupp. Pushing the limits of LTE: A survey on research enhancing the standard. *IEEE Access*, 1:51–62, 2013.
- [37] M. Taranetz, T. Blazek, T. Kropfreiter, M. K. Müller, S. Schwarz, and M. Rupp. Runtime precoding: Enabling multipoint transmission in lte-advanced system-level simulations. *IEEE Access*, 3:725–736, 2015. ISSN 2169-3536. doi: 10.1109/ACCESS.2015.2437903.